



MTSRF Project 3.7.9 – Remote Sensing
of GBR wide water quality:
RWQPP Marine Monitoring Program

Vittorio E. Brando, Thomas Schroeder, Arnold G. Dekker,
David Blondeau-Patissier

CSIRO Land & Water
20 November 2008

**Milestone Report for Reef Water Quality
Protection Plan (RWQPP) Marine Monitoring
Program**

CONTENTS

INTRODUCTION 6

Project objectives and methodology..... 6

SUMMARY OF THE RESULTS ACHIEVED FOR THIS MILESTONE 7

Improvements on the methods 7

 Atmospheric correction7

 Optical water quality retrieval.....7

Validation..... 7

Results 8

Management relevant remote sensing products to monitor water quality in GBR 8

Recommendations and future work 9

DETAILED DESCRIPTION OF THE RESULTS ACHIEVED FOR THIS MILESTONE 11

Improvements on the methods 11

 Atmospheric correction11

 Artificial neural network atmospheric correction algorithm development ..12

 Artificial neural network atmospheric correction algorithm validation and application13

Optical water quality retrieval 16

 Optical characterization of dry and wet season for the wet tropics16

 IOP and concentrations retrieval - LMI16

 Parameterization of LMI17

Algorithm validation 19

Management relevant remote sensing products to monitor water quality in GBR 22

Results 24

 Guide to interpreting the maps24

 The wet and dry season median maps for chlorophyll, suspended matter and vertical attenuation coefficient of light.24

 Comparison of the in situ data distributions of the long term monitoring plan with the remote sensing data distributions32

 Flood plume mapping38

ACKNOWLEDGMENTS..... 45

**APPENDIX B NOTES ON DETECTING TRICHODESMIUM SP. IN MERIS
IMAGERY 46**

List of Tables

Table 1 Project Targeted Activities (including out years)7
 Table 2 The final centroids identifying the most representative SIOP sets that were used in the regional algorithm parameterization of LMI_CLU4..... 17
 Table 3 Model II regression statistics for the measurements collected with 3 hours of the overpass. r is the Spearman correlation coefficient, RMSE the root mean square error22
 Table 4. Examples of potential application of remote sensing products addressing the main needs of the end users of spatially explicit water quality data.....23

List of Figures

Figure 1 Atmospheric correction failure: negative reflectances retrieved by NASA algorithm for the Mackay – Whitsundays, QLD – 22 February 2008. (red areas are the pixels with negative values, i.e where the NASA’s atmospheric correction algorithm failed) 11
 Figure 2: Scatter plots of the median reflectances of the MODIS Level2 product (left) and the proposed ANN atmospheric correction (right) compared to 31 in-situ reflectance measurements collected by GKSS, MUMM and CSIRO..... 14
 Figure 3: By comparison with in-situ reflectance measurements derived spectral slopes of RMSE (left) and MAPE (right) for the MODIS standard Level2 product generated with SeaDAS v5.1.1 (blue) and the proposed ANN algorithm (red)..... 14
 Figure 4: Comparison of SeaDAS v5.1.1 and ANN derived reflectance spectra for a MODIS Aqua scene acquired on 22 February 2008. 15
 Figure 5 Spatial distribution of the reflectance at 412 551 nm as derived by the ANN algorithm and NASA standard algorithm from a MODIS Aqua scene acquired on 22 February 2008 (black areas=masked pixels)..... 15
 Figure 6 aphy* spectra for LMI inversion in the parameterization for 2006 MMP report 18
 Figure 7 aphy* spectra for LMI inversion in the current version of the parameterization (LMI_CLU4)..... 18
 Figure 8 Effects of presence of Trichodesmium in the comparison of MODIS Aqua chlorophyll retrieval with in situ data. Chl_LMI_tricho are MODIS Aqua chlorophyll retrieval for data points with an associated record of presence of Trichodesmium. Chl_LMI_tricho_MERIS were data points with an associated record of absence of Trichodesmium for which the presence was confirmed using MERIS imagery.....20
 Figure 9: MODIS Aqua chlorophyll retrieval vs. in situ data. Only the measurements collected with 3 hours of the overpass were plotted. Number of matchups are 102 for LMI and 118 for gsm. The parameters for the regression lines are reported in Table 3.21
 Figure 10: MODIS Aqua chlorophyll retrieval vs. *in situ* data. Same as Figure 9, but with log-log scale to enhance the range between 0.1 and 1 $\mu\text{g L}^{-1}$21
 Figure 11. Chlorophyll Median maps for the dry and wet season for the Fitzroy Estuary – Keppel Bay region. Map a) (top panel) presents the median for the Dry Season 2007 (May - October), while map b) (bottom panel) presents the median for the Wet Season 2007/2008 (November 2007- April 2008). See text for annotation explanation.26
 Figure 12. CDOM Median maps for the dry and wet season for the Fitzroy Estuary –Keppel Bay region. Map a) (top panel) presents the median for the Dry Season 2007 (May - October), while map b) (bottom panel) presents the median for the Wet Season 2007/2008 (November 2007- April 2008). See text for annotation explanation.27
 Figure 13. Non-algal particulate matter (Nap as a measure of TSM) Median maps for the dry and wet season for the Fitzroy Estuary –Keppel Bay region. Map a) (top panel) presents the median for the Dry Season 2007 (May - October), while map b) (bottom panel) presents the median for the Wet Season 2007/2008 (November 2007- April 2008). See text for annotation explanation.....28

Figure 14. Vertical attenuation of light (K_d , as estimate of water clarity) Median maps for the dry and wet season for the Fitzroy Estuary –Keppel Bay region. Map a) (top panel) presents the median for the Dry Season 2007 (May - October), while map b) (bottom panel) presents the median for the Wet Season 2007/2008 (November 2007- April 2008). See text for annotation explanation.29

Figure 15. Secchi Depth (as estimate of water clarity) Median maps for the dry and wet season for the Fitzroy Estuary –Keppel Bay region. Map a) (top panel) presents the median for the Dry Season 2007 (May - October), while map b) (bottom panel) presents the median for the Wet Season 2007/2008 (November 2007- April 2008). See text for annotation explanation.30

Figure 16. Number of pixels used to calculate the Median maps (Figure 11 - Figure 15) for the dry and wet season for the Fitzroy Estuary –Keppel Bay region (). Map a) (top panel) presents the number of pixels available for the Dry Season 2007 (May - October), while map b) (bottom panel) presents the number of pixels available for the Wet Season 2007/2008 (November 2007- April 2008). See text for annotation explanation.31

Figure 17. Comparison of chlorophyll concentrations retrieved from MODIS-AQUA data with in-situ data from the GBR LTMP for the CAIRNS region. Figures a and b results for dry and wet season of 2005/2006. The nine box-whiskers plots are organised in three panels: in-situ data from the GBR LTMP; satellite-derived, time-series data of the pixel encompassing the in situ sites; and all satellite-derived, time-series data. The box-whiskers plots for coastal, inshore and offshore regions are presented in each panel.33

Figure 18. Comparison of chlorophyll concentrations retrieved from MODIS-AQUA data with in-situ data from the GBR LTMP for the Cape York region. Figures a and b results for dry and wet season of 2005/2006. The nine box-whiskers plots are organised in three panels: in-situ data from the GBR LTMP; satellite-derived, time-series data of the pixel encompassing the in situ sites; and all satellite-derived, time-series data. The box-whiskers plots for coastal, inshore and offshore regions are presented in each panel. Of the GBR LTM sites, site 483 was visited in the coastal region, and sites 489, 492, 493, 495, 511, and 521 in the offshore region, site 483 was visited only twice and the box-whiskers plot was not reported. Only sites 483, 489, 493, and 494 were in locations not masked by the reef or land mask in the satellite imagery.....34

Figure 19. Comparison of chlorophyll concentrations retrieved from MODIS-AQUA data with in-situ data from the GBR LTMP for the Burdekin region. Figures a and b results for dry and wet season of 2005/2006. The nine box-whiskers plots are organised in three panels: in-situ data from the GBR LTMP; satellite-derived, time-series data of the pixel encompassing the in situ sites; and all satellite-derived, time-series data. The box-whiskers plots for coastal, inshore and offshore regions are presented in each panel. Of the GBR LTM sites, site 523 was visited only twice in the inshore region and the box-whiskers plot was not reported.35

Figure 20. Comparison of chlorophyll concentrations retrieved from MODIS-AQUA data with in-situ data from the GBR LTMP for the Mackay region. Figures a and b results for dry and wet season of 2005/2006. The nine box-whiskers plots are organised in three panels: in-situ data from the GBR LTMP; satellite-derived, time-series data of the pixel encompassing the in situ sites; and all satellite-derived, time-series data. The box-whiskers plots for coastal, inshore and offshore regions are presented in each panel. Of the GBR LTM sites, sites 473 for the coastal region and 540, 541, 1444 in the offshore region were visited; site 473 was visited only twice during the dry season and the box-whiskers plot was not reported. Only sites 473, 474, 478, 479, 481 and 1445 were in locations not masked by the reef or land mask in the satellite imagery.36

Figure 21. Comparison of chlorophyll concentrations retrieved from MODIS-AQUA data with in-situ data from the GBR LTMP for the Fitzroy region. Figures a and b results for dry and wet season of 2005/2006. The nine box-whiskers plots are organised in three panels: in-situ data from the GBR LTMP; satellite-derived, time-series data of the pixel encompassing the in situ sites; and all satellite-derived, time-series data. The box-whiskers plots for coastal, inshore and offshore regions are presented in each panel. None of GBRLTM sites were located within the offshore region.....37

Figure 22. Chlorophyll Median maps for the wet season 2006/2007 (November 2006- April 2007) for the Fitzroy Estuary –Keppel Bay region. See text for annotation explanation.39

Figure 23. CDOM Median maps for the wet season 2006/2007 (November 2006- April 2007) for the Fitzroy Estuary –Keppel Bay region. See text for annotation explanation.39

Figure 24. Non-algal particulate matter (Nap as a measure of TSM) Median maps for the wet season 2006/2007 (November 2006- April 2007) for the Fitzroy Estuary –Keppel Bay region. See text for annotation explanation.40

Figure 25. Vertical attenuation of light (K_d , as estimate of water clarity) Median map for the wet season 2006/2007 (November 2006- April 2007) for the Fitzroy Estuary –Keppel Bay region. See text for annotation explanation.40

Figure 26. Secchi Depth (as estimate of water clarity) Median map for the wet season 2006/2007 (November 2006- April 2007) for the Fitzroy Estuary –Keppel Bay region. See text for annotation explanation.**Error! Bookmark not defined.**

Figure 22. Daily true colour images and CDOM maps for key dates during the 2008 flood event for the Fitzroy Estuary –Keppel Bay region. From top to bottom: 28 January 2008, 21 February 2008, 22 February 2008 and 7 march 2008. See text for annotation explanation. 41

Figure 27. Maps of the 75th percentiles for CDOM for the wet season 2006/2007 and 2007/2008 for the Fitzroy Estuary –Keppel Bay region. See text for annotation explanation.42

Figure 28. Maps of the 95th percentiles for CDOM for the wet season 2006/2007 and 2007/2008 for the Fitzroy Estuary –Keppel Bay region. See text for annotation explanation.43

Figure 29. Maps of Maximum retrieved value of CDOM for the wet season 2006/2007 and 2007/2008 for the Fitzroy Estuary –Keppel Bay region. See text for annotation explanation.44

Figure 30 MERIS L1 reduced resolution (i.e., 1 pixel = 1 km) composites of bands 775nm, 705nm and 681 nm showing the locations of five stations sampled near the Fitzroy estuary on 6th October 2004 (red circle, left panel). After applying a Gaussian stretch on the same image, the long, brown filaments are *Trichodesmium* sp. become visible (right panel). Stations codes are shown.46

Figure 31 MERIS radiance spectrum of the studied pixel (centre of the red cross) showing a continuous decrease in radiance from 412 and and 681 nm, followed by a positive slope between 681 and 705nm that identifies *Trichodesmium* sp..47

INTRODUCTION

Remote sensing derived information is a cost-effective method to determine spatial and temporal information on near-surface concentrations of suspended solids (as non-algal particulate matter), turbidity (as vertical attenuation of light coefficients K_d), chlorophyll a (CHL) and colored dissolved organic matter (CDOM) for the GBR. This is achieved through the acquisition, processing with regionally valid algorithms, validation and transmission of geo-corrected ocean colour imagery and data sets derived from MODIS imagery. This project will also include the development of new analytical tools for understanding the trends and anomalies of these waters (specifically wet season to dry season variability, river plume composition and extent and algal blooms) based on the characteristics of optical satellite remote sensing data.

Project objectives and methodology

Key Objectives the projects are :

To assess spatial and temporal changes in near-surface concentrations of suspended solids, turbidity, CDOM and chlorophyll a for the coastal and lagoonal waters of the Great Barrier Reef.

Develop improved algorithms for water quality and atmospheric correction for the waters of the GBR.

This project will be achieved through the acquisition, processing with regionally valid algorithms, validation and transmission of geo-corrected ocean colour imagery and data sets derived from MODIS imagery. It will need development of new analytical tools for understanding the trends and anomalies of these waters (specifically wet season to dry season variability, river plume composition and extent and algal blooms) based on the characteristics of optical satellite remote sensing data.

Objective	Targeted Activity	Completion Date
(a)	Acquire daily remotely sensed data of the Great Barrier Reef region over the period April 2007 – April 2008	May 2008
(a)	Process acquired data to provide summary images of chlorophyll a, total suspended matter (as non-algal particulate matter concentration), coloured dissolved organic matter (CDOM), and k_d . (for each of the 6 GBR NRM regions) monthly log means (and SD) or medians, and percentiles (wet and dry season comparison plus comparison to grab sampling) The temporal and spatial variation in the extent of available 2007/08 river flood plumes across the 6 GBR NRM regions (plume marked on pseudo true colour MODIS images, possibly supplemented by MERIS and SeaWiFS images).	August 2008
(a)	Development of trends and anomaly detection algorithms for GBR WHA based on existing long term MODIS data sets (in any case MODIS Aqua from 2002 launch date onwards; possibly augmented by MODIS Terra from 1999 onwards and SeaWiFS from 1997 onwards).	May 2009
(b)	Carry out opportunistic wet season flood field work for remote sensing validation	Feb 2008
(b)	Improve of wet season algorithms to be able to deal with extremely turbid river plumes entering the GBR waters whilst still assessing chlorophyll (to the limit of the noise in the remote sensing data).	November 2008
(b)	Improvement of atmospheric correction algorithms to enable near coastal quantitative water quality assessments from RS	May 2008

(b)	Validation of atmospheric correction algorithms to enable near coastal quantitative water quality assessments from RS	November 2008
(all)	Project Leader and/or other nominated personnel attend and contribute to synthesis and integration workshop, held in Townsville to present remote sensing GBR water quality data to enable collaborative completion of a synthesis and integration report.	September 2008
(all)	Contribute to the integrated report on the status of Great Barrier Reef Water Quality and ecosystem health.	November 2008

Table 1 Project Targeted Activities (including out years)

SUMMARY OF THE RESULTS ACHIEVED FOR THIS MILESTONE

Improvements on the methods

Atmospheric correction

The application of NASA's atmospheric correction algorithm as implemented in SeaDAS v5.1.1 systematically retrieves negative water-leaving radiances for the Great Barrier Reef coastal waters. A first step for accurate chlorophyll retrievals in Great Barrier Reef coastal waters was thus to develop of a new atmospheric correction algorithm. Our new MODIS atmospheric correction algorithm was developed by inverse modelling of radiative transfer (RT) calculations within a coupled ocean-atmosphere system by utilizing an artificial neural network (ANN) technique (Schroeder et al., 2008).

The proposed atmospheric correction scheme provides a significant improvement in accuracy for the retrieval of reflectance data from MODIS Terra/Aqua measurements. From match-up analysis within coastal waters an overall mean absolute percentage error of 17.5% within the spectral range of 412-748 nm was derived. Compared to NASA's standard atmospheric correction implemented in SeaDAS v5.1.1., the proposed neural network approach showed a significant improvement in accuracy, especially in the blue part of the spectrum (Schroeder et al., 2008).

Optical water quality retrieval

In previous years CSIRO's Environmental Earth Observation Group assessed the performance for the local conditions of coastal GBR waters of the seven NASA global Chlorophyll-a (CHL) algorithms implemented in SeaDAS (Qin et al., 2007). To improve the accuracy of chlorophyll and IOP estimates from MODIS AQUA data in GBR Lagoon coastal waters an enhancement of the Linear Matrix Inversion (LMI, Hoge and Lyon, 1996) was used to incorporate regional and seasonal knowledge of variability in the specific inherent optical properties of concentration specific light absorption and scattering encountered in GBR coastal waters (Brando et al 2008). The algorithm estimates simultaneously the concentration of Chlorophyll, Total suspended sediment, CDOM and the vertical attenuation coefficient, K_d .

For this study, to incorporate regional knowledge of specific IOPs, LMI was parameterized following the approach used in the previous MMP report (Appendix 1 pages A40- A-57, Schaffelke et al., 2006). Two adjustments on the optical properties of phytoplankton were made to the original parameterization.

Validation

The comparison of MODIS Aqua chlorophyll retrieval with *in situ* data showed that revised parameterization of regional algorithm coupled with the new Artificial Neural Network atmospheric correction led to a marked improvement since the previous report. Even though the correlation

coefficient was low, the slope regression coefficients for the LMI algorithm were close to the 1. The Bias for the MODIS Aqua chlorophyll retrievals by the LMI algorithm were nil but the percentage error was quite high (~110-120%).

The presence of *Trichodesmium* leads to a gross underestimation and overestimation of chlorophyll in the water column because of (sub-) surface expression and spatial heterogeneity. To overcome this issue an operational algorithm to identify *Trichodesmium* affected pixels for MODIS imagery should be implemented and then an inversion algorithm to estimate chlorophyll for pixels with a *Trichodesmium* expression should be developed.

The statistical distributions of the chlorophyll –a retrieved with the algorithm from MODIS-AQUA data were compared with the in-situ data from the GBR LTMP for each region for the wet and dry season 2005/2006. In general the box-whiskers plots show higher chlorophyll value expressed as medians and 25 to 75% percentiles for the in situ samples and the remote sensing estimates of the waters in the coastal region than for the waters in inshore region and the offshore region. Most of the times the ranges of the measured in situ samples fall within the ranges of the remotely sensed values

Results

The number of image pixels per pixel location available for calculating the median values for each season increased from 5 to 60 of the previous MMP report to from 30 to about 90 of this study. This reduction of pixels being dismissed because of atmospheric correction failure or because the error between modelled and measured spectra was too high is a direct result of the implementation of the new Artificial neural network atmospheric correction.

The wet and dry season median maps of Chlorophyll-a, coloured dissolved organic matter (CDOM) and non-algal particulate matter (as a measure of total suspended matter) showed a clear difference in patterns and values between the dry and wet seasons 2007/2008. When compared with Median maps for the wet season 2006/2007, the Median maps for the Fitzroy Estuary – Keppel Bay region for the Wet Season 2007/2008 showed a larger extent of the coastal influence for all the mapped variables.

The median maps of water clarity expressed as Secchi Depth for the Fitzroy Estuary –Keppel Bay region show similar patterns to the maps of vertical attenuation of light. The Secchi Depth product is still in development phase and should be validated using the water quality data sets used in recent studies on the spatial and temporal patterns of water quality of the Great Barrier Reef (De'ath 2007, 2008).

The extent of the flood event occurred in the Fitzroy River in January-February 2008 was characterized comparing the maps of the 75th and 95th percentiles and the maximum retrieved CDOM values of the 2007/2008 wet season to the previous year when no flow event occurred. The values of CDOM in the 75th percentiles map for 2008 were comparable in magnitude with the 95th percentiles of the 2007 wet season. The map of the maximum retrieved CDOM values for 2008 clearly showed the lobes of high concentrations of dissolved materials that were observed from the daily imagery and in the field during the late January and mid February peak events

In all likelihood further improvements possible within a year will enhance the confidence in the remote sensing estimates to the degree that remote sensing can become the prime detection and monitoring tool for chlorophyll, CDOM, TSM and K_d estimates in the GBRWHA.

Management relevant remote sensing products to monitor water quality in GBR

If environmental managers in the GBRWHA are to take full advantage of remote sensing capabilities then products that translate remotely-sensed scenes into useful information for managers are required.

The main needs of the end users of spatially explicit water quality data can be summarised as:

- Status description and trend detection

- Characteristics of river plumes such as influence on high value assets, Observation of extent of influence of river plumes, definition of areas of Water Quality risk
- Compliance against targets: over spatial areas or specific assets, during river plumes, or risk hotspots
- Link monitoring & modelling – RS provides monitoring components. RS can be used to validate receiving water model with RS data.

To enable the adoption of remote sensing products in the adaptive management of GBR coastal waters it is imperative that these products are:

- suitable for use in media, web and report cards;
- presented in a manner that can be interpreted and used by managers (training and education loop between providers and users is needed);
- accompanied by a user guide for the range of products;

CSIRO's Environmental Earth Observation Group developed a software suite to produce from daily remote sensed data a number of derived products suited to the specific needs of end-users, in a number of outputs, including maps, animations, statistical compliance assessments and alert or anomaly systems. The software suite enables the production of maps of:

- Min, Max, Median, Logmean, Mean, STD of Chlorophyll, TSM, CDOM and Kd for the GBRWHA.
- Maps of 5th, 25th, 75th and 95th of Chlorophyll, TSM, CDOM and Kd for the GBRWHA.
- Weekly, monthly, seasonal, and yearly and long term statistics
- Assessment of the exceedance of water quality guidelines for water quality variables.

Comment [bra372 1]: this text is new

All the maps and comparisons with in situ data presented in this report were produced using the above mentioned software suite. The software suite will be made available in the coming future to the GBRWHA management and research community.

Recommendations and future work

Comprehensive wet season studies carried out by CSIRO's Environmental Earth Observation Group with DEWHA co-funding, has shown that considerable differences in optical properties and concentrations are found between the dry and wet season for the GBR lagoonal waters. In order to incorporate seasonal knowledge of variability in the specific inherent optical properties in the algorithms, a new comprehensive statistical analysis should be performed to include the optical characterizations carried out in the last two years, in particular the flood waters of the Fitzroy River in Keppel Bay (February 2008) and the wet season sampling of the wet tropics (April 2008).

To strengthen the validation of remote sensing data, the validation database should be extended to include water quality data sets used in recent studies on the spatial and temporal patterns of water quality of the Great Barrier Reef (De'ath 2007, 2008). The Secchi depth (m) database would allow a direct validation the Secchi Depth estimates done from remote sensing data.

CSIRO's Environmental Earth Observation Group is currently setting up the Lucinda Jetty Coastal Observatory (LJCO), as part of the Australian National Mooring Network, one the facilities of Australia's Integrated Marine Observing System (IMOS). LJCO aims to provide valuable data in tropical Queensland coastal waters to unravel the inaccuracies in remotely-sensed satellite ocean colour products due to the optical complexity in coastal waters and the overlying atmosphere. The LJCO data stream will increase the number of satellite vs. in situ match-ups assessment of normalized water-leaving radiances, water inherent optical properties and aerosol optical properties.

In the meanwhile, AIMS is leading the setup of GBROOS (Great Barrier Reef Ocean Observing System). Several autonomous water quality loggers will be deployed in GBR waters. The GBROOS data sets should also be used to evaluate and improve the accuracy of remote sensing retrieval.

To provide further information on the spatial variability of water quality in the GBR waters the deployment of automated measuring systems on "Ships of Opportunity" should be considered. Ships

should be fitted with automated sensors which record the water quality parameters such as temperature, salinity, turbidity, oxygen, nutrients and chlorophyll during the trip. Such systems are already used for operational observations of water quality in different regions of the world.

The maps of the 75th and 95th percentiles and the maximum retrieved CDOM values for the wet season were made available to Michelle Devlin (ACTFR) to carry out further research activities to within another MTSRF project. Further collaboration with this group in the near future will enable a comprehensive characterization of the extent of the flood event occurred in the Fitzroy River in January-February 2008 as well as other flood events occurring in the region.

CSIRO's Environmental Earth Observation Group is currently exploring avenues for assimilation of satellite observational data with biogeochemical and sediment transport models in Keppel Bay, within a collaborative project funded by CSIRO's "Water for a Healthy Country" Flagship. An improved model for light attenuation based on the specific optical characteristics of dissolved and particulate substances in Keppel Bay was developed based on the local optical measurements and remotely sensed light attenuation estimate. Currently the group is evaluating the use of satellite observations to supplement in situ data to improve calibration and parameterisation of the model for the estimate of fluxes to the GBR. Assimilation of satellite observations with biogeochemical and sediment transport models is likely to become increasingly important in the near future, as it combines the merits of both tools.

In the last few years CSIRO's Environmental Earth Observation Group has been investigating with DEWHA funding how to evaluate water quality compliance for the GBR using chlorophyll retrieved from remote sensing. Further research is needed to incorporate the latest water body delineations (De'ath 2007, 2008) and trigger values definition according to the draft GBR water quality guidelines so that compliance assessment procedure can be incorporated in the routine monitoring and assessment of trends for GBR water quality reporting.

In the coming year, the methods for deriving management relevant products from remote sensing data developed CSIRO's Environmental Earth Observation Group will be contributed to the Reef Atlas to provide input into GBR water quality reporting such as the GBRMPA Outlook report and Reef Report card.

DETAILED DESCRIPTION OF THE RESULTS ACHIEVED FOR THIS MILESTONE

Improvements on the methods

In this work we coupled two physics-based inversion algorithms with the objective to improve the accuracy of chlorophyll and IOP estimates from MODIS AQUA data in GBR Lagoon coastal waters. In a first step, an atmospheric correction algorithm based on inverse modelling of radiative transfer simulations and Artificial Neural Network (ANN) inversion, derives the remote sensing reflectance at mean sea level (Schroeder et al. 2008). Then, the inherent optical properties and the concentrations of the optically active constituents, namely Chlorophyll-a, non-algal particulate matter (NAP) and coloured dissolved organic matter CDOM, were retrieved using an enhancement of the Linear Matrix Inversion (LMI, Hoge and Lyon, 1996) that incorporates regional and seasonal knowledge of specific IOPs (Brando et al 2008).

Atmospheric correction

The application of NASA's atmospheric correction algorithm as implemented in SeaDAS v5.1.1 systematically retrieves negative water-leaving radiances for the Great Barrier Reef coastal waters (Figure 1). A first step for accurate chlorophyll retrievals in Great Barrier Reef coastal waters was thus to develop of a new atmospheric correction algorithm. Our new MODIS atmospheric correction algorithm was developed by inverse modelling of radiative transfer (RT) calculations within a coupled ocean-atmosphere system by utilizing an artificial neural network (ANN) technique.

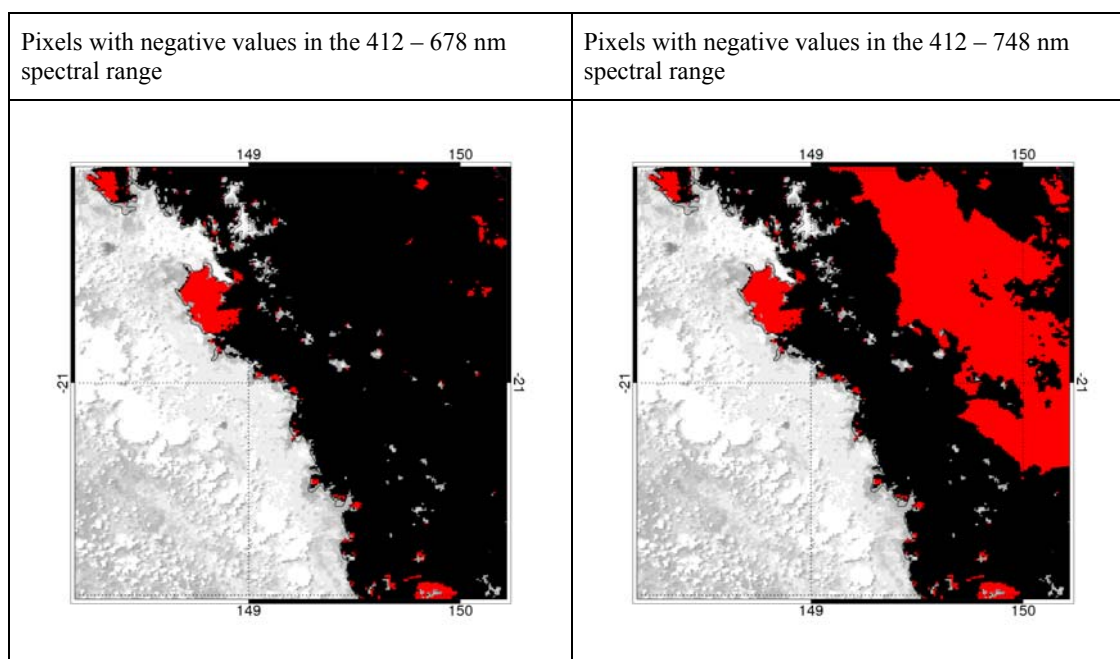


Figure 1 Atmospheric correction failure: negative reflectances retrieved by NASA algorithm for the Mackay – Whitsundays, QLD – 22 February 2008. (red areas are the pixels with negative values, i.e where the NASA's atmospheric correction algorithm failed)

Artificial neural network atmospheric correction algorithm development

Our new MODIS atmospheric correction algorithm was developed by inverse modelling of radiative transfer (RT) calculations within a coupled ocean–atmosphere system by utilizing an artificial neural network (ANN) technique. The algorithm was implemented similar to an approach developed by Schroeder et al. (2007a) for MERIS, but with a different inverse model capable of generating more complex network architectures. Within this model-based approach, ANNs were found well suited to deal with the optical-complex coastal waters because multilayer feed-forward networks with nonlinear transfer functions, as implemented in this work, are known as universal function approximators (Hornik et al. 1989).

By utilizing an established and validated radiative transfer code as a forward model (Fischer and Grassl 1984; Fell and Fischer 2001), a large data base of azimuthally resolved upward radiances in the MODIS channels at the Bottom-Of-Atmosphere (BOA) and at the Top-Of-Atmosphere (TOA) was generated for a variety of sun and observing geometries as well as different types of atmospheric and oceanic constituents. Various ANNs serving as inverse models were trained under a supervised learning procedure by applying a non-linear optimisation routine on the basis of a randomly selected data subset of 100.000 spectra taken from the simulated data base. A detailed description of all inputs to the RT model can be found in Schroeder et al. 2007a, 2007b.

The inverse models are fully connected feed-forward networks with one or two hidden layers of neurons. Their free parameters (so called weights) were estimated during a supervised learning procedure based on a least-mean-squares approach: samples from the randomly created subset were presented to the networks and their outputs compared against the expected outputs as given in the data base. The estimation error, i.e. the sum of squared differences between the network's outputs and the expected outputs, was used to adapt the parameters of the networks using a Limited Memory Broyden-Fletcher-Goldfarb-Shanno (L-BFGS) algorithm, a variable metric method, which is sometimes called the "quasi-Newton" method. This has to be done sequentially for all data of the subset until the total estimation error is minimal. The network applied here consists of three and four layers of neurons, an input layer, one or two hidden layers and an output layer, and is thus able to perform a highly non-linear function approximation (Bishop 1995). While the number of neurons for the input and output layers is fixed by the dimension of the problem under investigation, the optimum number of neurons for the hidden layers has to be optimized by the training of different networks. As there is no theoretical model to simply fix the optimum architecture, it has to be found iteratively by varying the number of neurons in the hidden layers. However, over-fitting occurs if too many neurons are chosen. The network then loses its power of generalization, which results in interpolation deficiencies, and the computation time increases. If too few hidden neurons are used, however, the error function may be minimized poorly (Bishop 1995). It is also important that the performance of different input scaling and noise levels are tested to derive an optimum network architecture.

In total 138 different networks were trained on basis of the simulated subset by applying different scaling and noise levels to the inputs as well as having the option of outputting additional aerosol optical thickness data. The learning was stopped for all networks after 1.000 iterations with the full subset of 100.000 simulated vectors. A single input vector contains the complete MODIS TOA reflectance spectrum of the bands 8-16, the sun and observing geometry and the surface pressure. The associated output vector consists of the reflectance spectrum at mean sea level (MSL) for the MODIS bands 8-15 (412-748 nm) with the output option of additional aerosol optical thickness data. At the end of the training phase the accuracy of each network was accessed by inverting „real-world“ MODIS data and comparing the outputs against in-situ data. Therefore, a match-up data base was compiled containing in-situ above water reflectance measurements collected by the GKSS Institute for Coastal Research and the Management Unit of the North Sea Mathematical Models (MUMM) during various MERIS Cal/Val field campaigns in North Sea turbid waters and by CSIRO in coastal waters of the Great Barrier Reef. The reflectances were measured according to the REVAMP protocols (Tilstone, 2002) using Trios RAMSES and SIMBADA spectrometers. The match-up criteria selected within this work was to allow a maximum time difference of ± 60 min to the satellite over pass with all match-up area pixels not flagged by LAND, CLOUD/ICE or HIGHGLINT. From more than hundred

in-situ spectra 31 finally met these criteria and were selected with their associated satellite data as match-up data set.

The performance of a first series of 72 different 3-layer MLP networks was assessed by inverting the match-up data set. These networks were trained with and without applying signal-dependent Gaussian noise to the simulated inputs in combination with and without decorrelating the input spectra by applying a principal component analysis (PCA) and with and without additional AOT outputs. The hidden layer neurons for these networks were varied between 20 and 60 in steps of 5. Applying a PCA helped the networks to reduce the BIAS and adding noise helped to reduce the absolute overall error measured as the root mean squared error (RMSE). Including additional outputs for the AOT did not result in an accuracy decrease in the reflectance data.

Based on these findings a second series of 15 networks were trained using the architecture of the best performing network from the first series by not varying any neurons, but by applying a combination of varying noise levels to the inputs. The signal-dependent, Gaussian noise added to the simulated TOA reflectances was varied between 0.2% and 1% in steps of 0.2% in combination with noise variations of 0.001%, 0.01% and 0.1% for the geometry parameters, while keeping a fixed noise level of 2% for the pressure data. By inverting the match-up database the optimum noise level was found to be 0.8% for the TOA reflectances in combination with 0.1% for the geometry inputs. This optimum noise level was used in combination with a PCA and AOT outputs to train a final series of fifteen 3-layer MLPs in varying the hidden layer neurons between 20 and 90 in steps of 5.

To analyse the impact of a further hidden layer a final series of 36 networks were trained using the previously accessed optimum noise level in combination with a PCA and AOT outputs and varying the hidden layer neurons between 15 and 40 in steps of 5 and permuting them. When inverting the match-up data set the overall accuracy of these 4-layer networks did not improve compared to the 3-layer MLPs.

Artificial neural network atmospheric correction algorithm validation and application

The best overall performance was achieved by a 3-layer network with 20 neurons for the hidden layer using PCA for input spectra decorrelation and AOTs as additional outputs. Figure 2 shows the scatter plots of the in-situ reflectance measurements against the median reflectance values derived from the SeaDAS v5.1.1 atmospheric correction output and the values obtained from the ANN correction scheme. We found a lower RMSE of 0.0035, a lower BIAS of 0.0015 and a higher correlation of 0.98 for the proposed ANN algorithm compared to the SeaDAS output, with an overall RMSE of 0.0058 with a BIAS of 0.0029 and a correlation of 0.95. At four stations in North Sea turbid waters SeaDAS atmospheric correction retrieved negative reflectances at 412 nm from the match-up data (Figure 2). The error bars in Figure 2 indicate the simple standard deviation of the reflectances within the 3 x 3 pixel match-up area and of the in-situ measurements.

The spectral error show the largest differences in the blue part of the spectrum for both algorithms (Figure 3), where the SeaDAS atmospherically corrected data resulted in a mean absolute percentage error (MAPE) of up to 48% compared to 19% for the ANN algorithm.

The performance of the ANN algorithm is demonstrated and illustrated by comparing selected reflectance spectra with the reflectance output of SeaDAS v5.1.1 for a MODIS Aqua scene acquired on 22 February 2008 covering the Mackay – Whitsundays (Figure 4). Spectra from off-shore areas are in good agreement, while SeaDAS fails for most of the near-shore coastal areas by retrieving negative spectra.

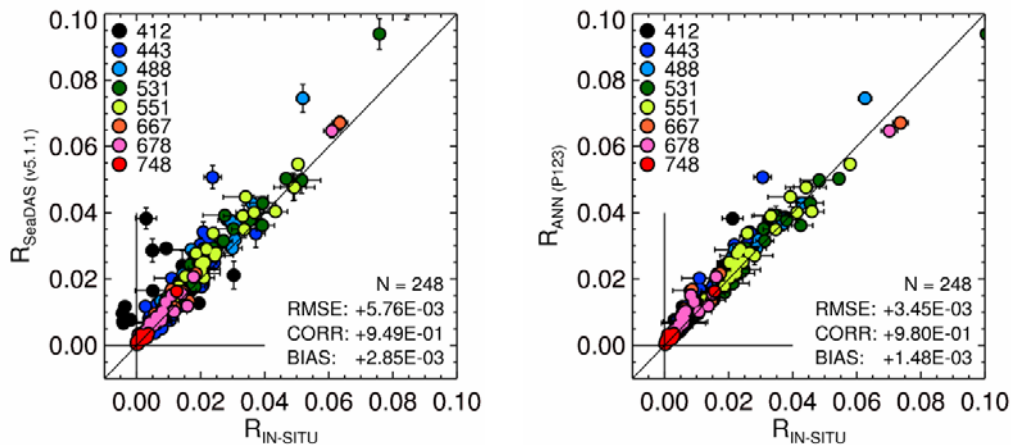


Figure 2: Scatter plots of the median reflectances of the MODIS Level2 product (left) and the proposed ANN atmospheric correction (right) compared to 31 in-situ reflectance measurements collected by GKSS, MUMM and CSIRO.

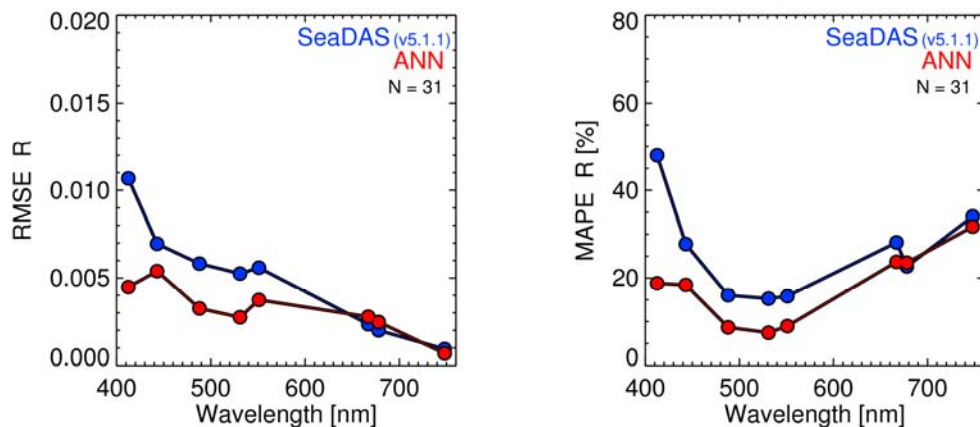


Figure 3: By comparison with in-situ reflectance measurements derived spectral slopes of RMSE (left) and MAPE (right) for the MODIS standard Level2 product generated with SeaDAS v5.1.1 (blue) and the proposed ANN algorithm (red).

To further illustrate the performance of the proposed ANN algorithm we shows map of the derived spatial reflectance distribution (Figure 5) for a MODIS Aqua scene acquired on 22 February 2008 covering the Mackay – Whitsundays coastal waters for the wavelengths 412 in comparison with the NASA’s atmospheric correction algorithm Higher TSM and CDOM concentrations can be associated with the near coastal waters of Repulse Bay causing negative reflectance values at 412 nm.

The proposed atmospheric correction scheme provides a significant improvement in accuracy for the retrieval of reflectance data from MODIS Terra/Aqua measurements. From match-up analysis within coastal waters an overall mean absolute percentage error of 17.5% within the spectral range of 412-748 nm was derived. Compared to NASA’s standard atmospheric correction implemented in SeaDAS v5.1.1., the proposed neural network approach showed a significant improvement in accuracy, especially in the blue part of the spectrum.

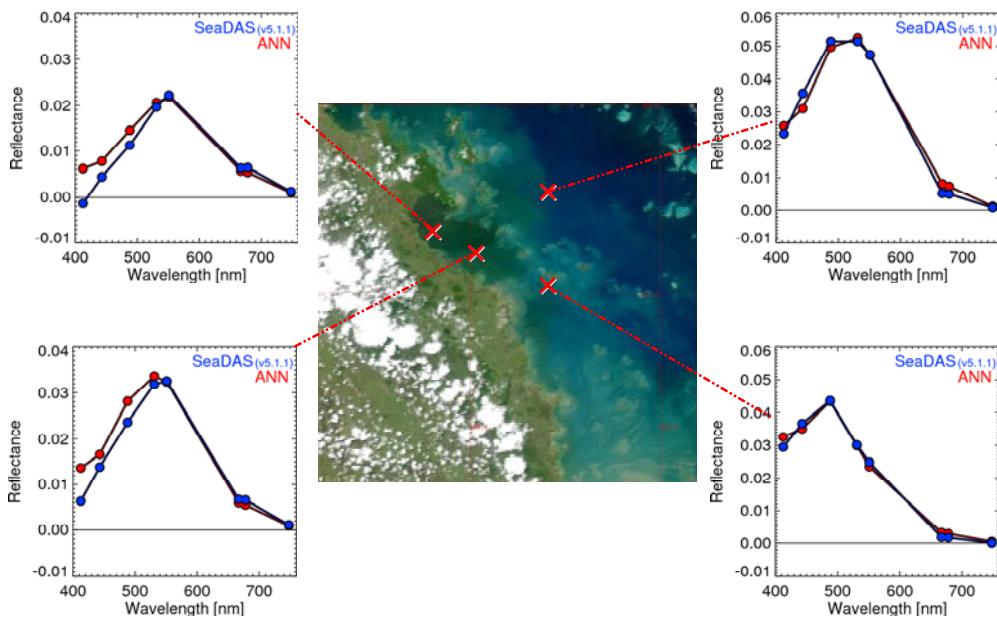


Figure 4: Comparison of SeaDAS v5.1.1 and ANN derived reflectance spectra for a MODIS Aqua scene acquired on 22 February 2008.

ANN atmospheric correction
 Reflectance at 412 nm

NASA standard atmospheric correction
 Reflectance at 412 nm

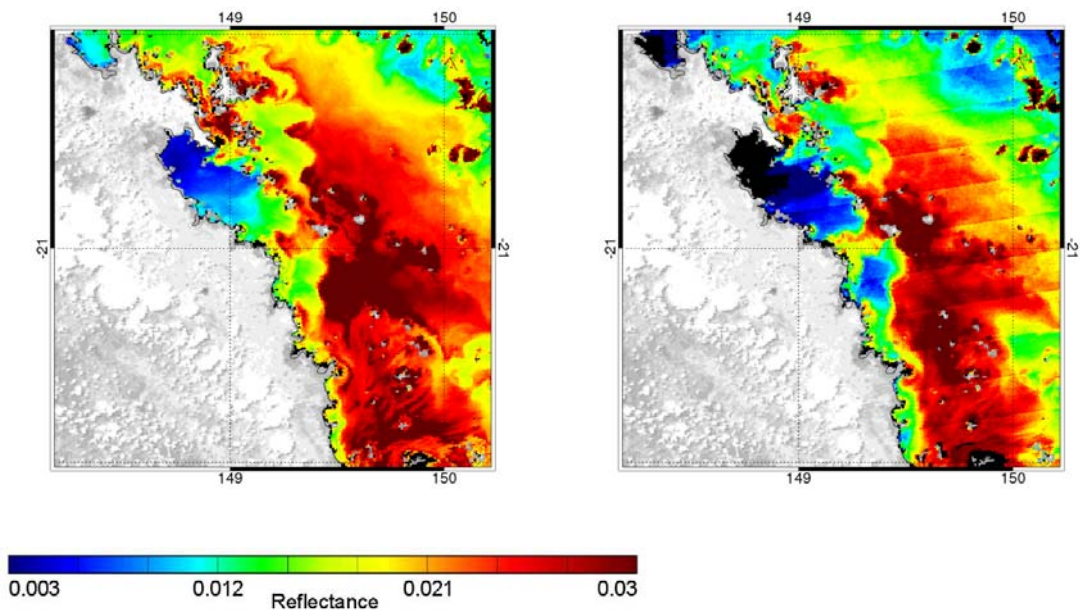


Figure 5 Spatial distribution of the reflectance at 412 551 nm as derived by the ANN algorithm and NASA standard algorithm from a MODIS Aqua scene acquired on 22 February 2008 (black areas=masked pixels).

Optical water quality retrieval

In previous years CSIRO's Environmental Earth Observation Group assessed the performance for the local conditions of coastal GBR waters of the seven NASA global Chlorophyll-a (CHL) algorithms implemented in SeaDAS. The accuracy of CHL retrieval for the seven empirical and semi-analytical algorithms generally degraded rapidly with increasing coloured dissolved organic matter (CDOM) and non-algal particulate matter (NAP) concentrations (Qin et al., 2007). The level of disagreement is at least twofold for concentrations of chlorophyll above $2 \mu\text{g L}^{-1}$. The gsm01 (Maritorena et al., 2002) algorithm was shown to work relatively better in the widest range of CDOM and NAP concentrations, while the Carder (Carder et al., 2003) algorithm has the highest accuracy for low CDOM and NAP concentrations. For the retrieval of bulk IOP, Qin et al. (2007) found that the three semi-analytical algorithms Carder, gsm01 and QAA seem unable to break down the total absorption coefficient, a , into its components, a_{ph} (phytoplankton) and a_{dg} (CDOM + NAP). This is probably because the three algorithms used a_{dg} slopes (QAA: 0.015, gsm01: 0.0206 and Carder: 0.0225) that are different than the values of S_{NAP} and S_{CDOM} found in the GBR coastal waters.

Optical characterization of dry and wet season for the wet tropics

To characterize the regional and seasonal variability in optical properties in GBR coastal waters between Cairns ($\sim 16.8^\circ\text{S}$) and Townsville ($\sim 18.8^\circ\text{S}$), two field campaigns were conducted during the austral dry (19-26 September 2007) and wet (18-23 April 2008) seasons with DEWHA co-funding. The study region was located in the Northern GBRL and extended from Trinity Bay ($\sim 16.5^\circ\text{S}$) in the north to Halifax Bay ($\sim 19^\circ\text{S}$) in the south and from the coast seawards to the middle shelf edge. The study area includes the coastal waters of Far North Queensland and is influenced by several rivers (Barron, Russell-Mulgrave River, Johnstone, Tully, Murray and Herbert rivers and Hinchinbrook Channel). Wet season sampling followed monsoonal activity that resulted in significant riverine discharge to the GBR coastal waters.

(Brando et al., 2008) (attached as Appendix A) have shown that considerable differences in optical properties and concentrations are found between the dry and wet season for the GBR lagoonal waters.

IOP and concentrations retrieval - LMI

To improve the accuracy of chlorophyll and IOP estimates from MODIS AQUA data in GBR Lagoon coastal waters, in this project an enhancement of the Linear Matrix Inversion (LMI, Hoge and Lyon, 1996) was used to incorporate regional and seasonal knowledge of variability in the specific inherent optical properties of concentration specific light absorption and scattering encountered in GBR coastal waters. The algorithm estimates simultaneously the concentration of Chlorophyll, Total suspended sediment, CDOM and the water clarity expressed both as vertical attenuation coefficient (K_d) and as Secchi Depth.

LMI has been already successfully applied to retrieve the concentrations of the optically active constituents in inland and coastal waters with hyperspectral data (Brando and Dekker, 2003; Giardino et al., 2007; Hoogenboom et al., 1998). This algorithm was adapted to MODIS for the Fitzroy River Estuary Keppel Bay (southern GBR) (Brando et al., 2006b; Brando et al., 2007) and applied to the MODIS-AQUA data for the whole GBRWHA (Brando et al., 2006a; Schaffelke et al., 2006). The LMI method as outlined here uses the below-water remote sensing reflectance spectrum of the eight MODIS bands 8-15 (412-748 nm) as input to a semi-analytical model developed by Gordon et al. (1988) to simultaneously derive the three optically active constituents in an algebraic manner.

One of the major weaknesses of the LMI is the difficulty of parameterising a stable spectral shape for each SIOP to reflect the natural variability (Lyon and Hoge, 2006). To overcome this, Wang et al. (2005) made use of an over-determined system (3×4 , $\lambda = 410, 440, 490$ and 550 nm) to explore the observed range of variability of the IOP shape factors. In this study, to incorporate regional knowledge of specific IOPs, the imagery inversion was performed while varying the SIOP shape parameters

through a series of unique combinations of the shape parameters, i.e. SIOP sets. Each SIOP set correspond to a complete set of SIOP shape parameters ($a_{phy}^*(\lambda)$, S_{CDOM} , $a_{NAP}^*(440)$, S_{NAP} , $b_{pphy}^*(555)$, γ_{phy} , $b_{bNAP}^*(555)$, γ_{NAP}) as they were measured concurrently at a single station during a cruise. With this approach, no a priori assumptions are made on the locations of specific water types in the satellite imagery and unnatural combinations of the shape factors are avoided. The SIOP set, the IOPs and concentrations values associated with the best optical closure are retained for each pixel and used for the output maps.

The optical closure is measured with *relRMSE*, the relative Root Means Square Error between the input remote sensing reflectance and the inverse-forward simulated reflectance calculated for each input spectrum. *relRMSE* provides a level of confidence of water quality parameter estimates. If the value of *relRMSE* exceeds a threshold, or if the retrieved concentrations are negative, or if one or more of the spectral bands of the image gives anomalous values (perhaps due to sun glint or some atmospheric haze etc.) then the pixel is flagged as not mapped.

Parameterization of LMI

For this study, to incorporate regional knowledge of specific IOPs, LMI was parameterize following the approach used in the previous MMP report (Appendix 1 pages A40- A-57, Schaffelke et al., 2006). The most relevant SIOP sets of the GRBWHA, that adequately represented the full range of SIOPs measured from Cape Tribulation down to Port Curtis, were selected through a rigorous QA/QC and subsequent statistical analysis of the in situ datasets over the period 2002-2005.

Two adjustments were made to the original parameterization carried out in for the 2006 MMP report: bb_phy_555nm was adjusted to reflected new literature values and the a_{phy}^* spectrum was fixed to only value for the whole GRBWHA (Figure 7) to avoid the contamination in the UV-blue and NIR ends of the spectrum by residual non algal particulate absorption that occurred for some of the sites in the previous parameterization (Figure 6).

The final centroids for each cluster are listed in Table 2 with all the values needed to parameterize LMI algorithm to estimate simultaneously the concentration of Chlorophyll, Total suspended sediment, CDOM and the water clarity expressed both as vertical attenuation coefficient (K_d) and as Secchi Depth. This version of the LMI parameterization was labelled LMI_CLU4.

A new statistical analysis comprehensive of Hierarchical clustering, Principal Component Analysis and Multi-Dimensional Scaling, should be performed to incorporate the new optical characterizations carried out in the last two years, in particular the flood waters of the Fitzroy River in Keppel Bay (February 2008) and the wet season sampling of the wet tropics (April 2008).

Table 2 The final centroids identifying the most representative SIOP sets that were used in the regional algorithm parameterization of LMI_CLU4.

Cluster	Site	bb_phy_slope	Bb_phy_555nm	a_cdom_slope	a_tr_slope	a_tr_440nm	bb_tr_slop	
1	AS05_WQN026	0.6649	0.0006	0.0336	0.0115	0.0188	0.6649	
2	MD_7D	0.7735	0.0006	0.0171	0.0119	0.0401	0.7735	
3	FK30	0.9882	0.0006	0.0146	0.0136	0.0391	0.9882	
4	FK35	0.421	0.0006	0.0116	0.0099	0.0281	0.421	
5	FK2-30	0.6065	0.0006	0.0181	0.0148	0.0271	0.6065	
6	FK2-23	0.8579	0.0006	0.0192	0.0118	0.0438	0.8579	
7	AA05_WQS008	0.7859	0.0006	0.012	0.011	0.0029	0.7859	
8	MD_15D	0.8393	0.0006	0.0144	0.0115	0.0266	0.8393	
9	AA05_WQS015	0.6003	0.0006	0.0105	0.0119	0.0057	0.6003	
10	AO02_SAT0021	1.3086	0.0006	0.0145	0.0124	0.0118	1.3086	

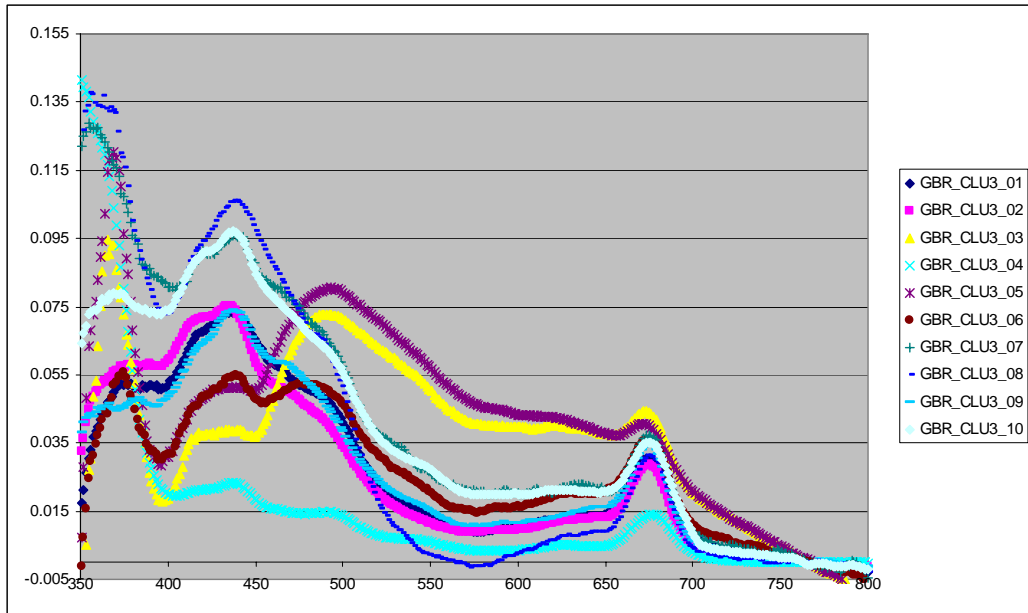


Figure 6 aphy* spectra for LMI inversion in the parameterization for 2006 MMP report

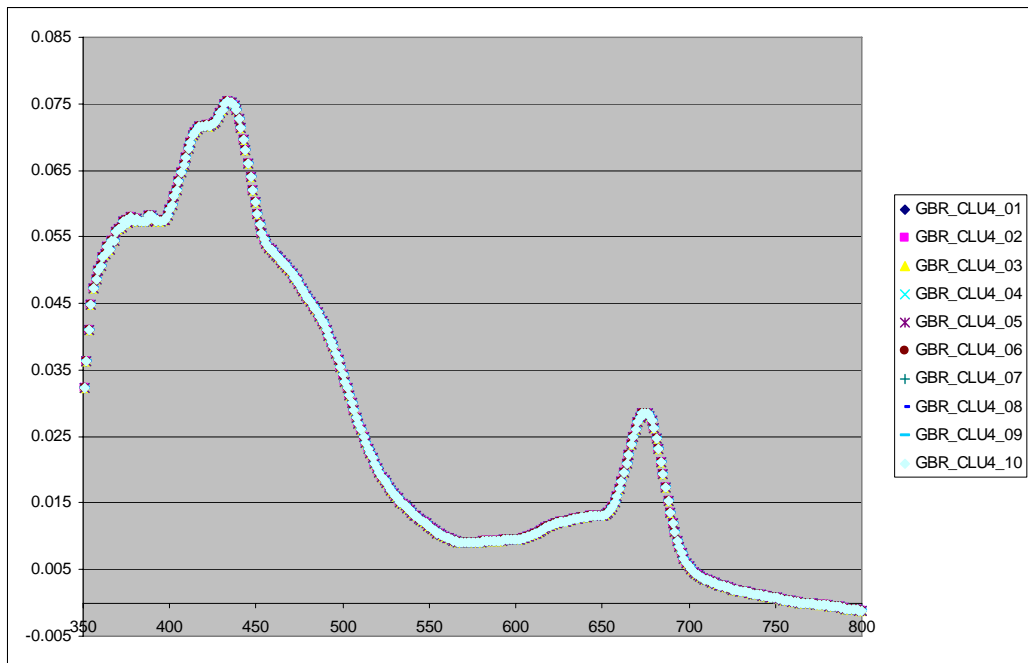


Figure 7 aphy* spectra for LMI inversion in the current version of the parameterization (LMI_CLU4).

Algorithm validation

For validation purposes the only data set that was independently available from the remote sensing algorithm development is the GBR Long Term Monitoring Program (GBR-LTMP) dataset. The GBR-LTMP dataset includes chlorophyll measurements going back as far as 1992 (thus including the start of the first contemporary ocean colour sensor SeaWiFS, launched in 1997).

This monitoring program was designed to monitor water quality status at regional spatial scales (Brodie et al 2007). The sampling stations for GBR-LTMP were situated some distance (~1-2 km) from the edge of nearby reefs to avoid confounding influences from biological activity on the reef itself (Brodie et al 2007). Chlorophyll and phaeophytin concentrations were determined fluorometrically, and a suite of site variables (water depth, presence of *Trichodesmium* and weather conditions) was measured to aid interpretation of the chlorophyll a data (Brodie et al 2007).

Chlorophyll data from the Cairns transect of collected by Miles Furnas and co-workers (AIMS) between 1988 and 2006 were also added to the validation database.

The GBR LTMP measurements were not designed for remote sensing validation purposes and thus the sampling protocols do not follow remote sensing validation guidelines (e.g minimum distance of 5 km from land or islands, HPLC estimate of chlorophyll a, etc.). For this reason, in this work this data set will be used to assess the suitability more than the absolute validity of the remote sensing data.

The GBR-LTMP chlorophyll data were used to evaluate the CHL_LMI_CLU4 product as well as CHL_gsm, as the gsm01 (Maritorena et al., 2002) algorithm was shown to work relatively better in the widest range of CDOM and NAP concentrations for these coastal waters (Qin et al., 2007). For this comparison, we extracted from the remote sensing data the average value of the nine pixels (a square of 3x3 pixels) centred at the GPS location of the in situ measurements, for each available date. The reason for this was that the long-term in situ chlorophyll data is presented as being measured at exactly the same location since 1992 whereas in reality wind and wave conditions cause the boat to be placed at different locations in the lee of the islands for safety. In addition, the time of the measurement was not coincidental with the satellite overpass and thus the water sampled by the in situ program may not have been in the same location as when the satellite passed over. Another reason for selecting a 3x3 pixel area is that it enables the estimate the standard deviation of the retrieval to be compared with the standard deviation of the *in situ* data. Unfortunately it should also be realised that the GBR-LTMP sample is of a few litres of water only, whereas the MODIS pixels are 1 km x 1 km (and then averaged over 3x3 pixels) to 9 km². The variability across this area is much better captured by the MODIS imagery. All the above qualifications of the validation method should be taken into consideration when interpreting these results.

As a result of the matchup analysis ~350 of a total ~3300 in situ data points were collected the same day of the overpass when the satellite data contained good quality data, i.e. at least one of the nine pixels was water (i.e. not masked as land or reef), free of cloud or glint contamination, the atmospheric correction was successful and the error between modelled and measured spectra was deemed to be acceptable. The *in situ* data with an associated record of presence of *Trichodesmium* were removed from this analysis as the presence of *Trichodesmium* leads to a gross underestimation and overestimation of chlorophyll in the water column because of (sub-) surface expression and spatial heterogeneity (Figure 8). Some data points where the absence of *Trichodesmium* was recorded but the satellite chlorophyll estimate were grossly underestimating the in situ data were removed after identifying the occurrence of *Trichodesmium* with the aid of MERIS imagery (Figure 8).

The principles of the method applied to MERIS imagery are described in Appendix B. Since this method cannot be applied directly to MODIS imagery, an operational algorithm to identify *Trichodesmium* affected pixels for MODIS imagery should be developed and implemented and then an inversion algorithm to estimate chlorophyll for pixels with a *Trichodesmium* expression should be developed.

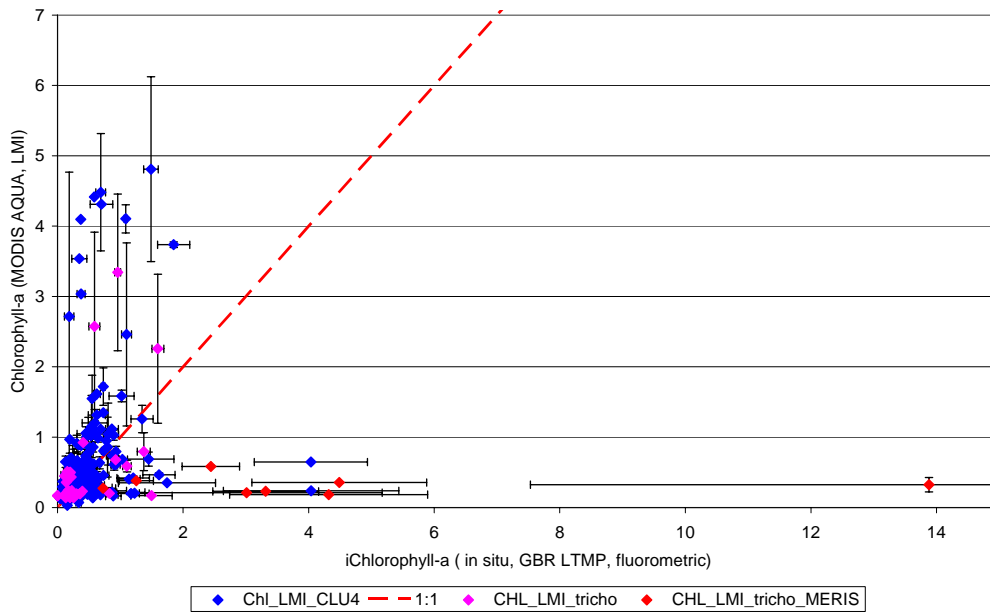


Figure 8 Effects of presence of Trichodesmium in the comparison of MODIS Aqua chlorophyll retrieval with in situ data. ChL_LMI_tricho are MODIS Aqua chlorophyll retrieval for data points with an associated record of presence of Trichodesmium. ChL_LMI_tricho_MERIS were data points with an associated record of absence of Trichodesmium for which the presence was confirmed using MERIS imagery.

After removing Trichodesmium affected data points, only the measurements collected within 3 hours of the overpass were analysed. Number of matchups was similar for LMI and gsm (102 and 118 respectively). Figure 9 and Figure 10 present the results of the MODIS Aqua chlorophyll retrieval comparison with *in situ* data in linear and logarithmic scale. A Reduced Major Axis regression (Model II, Sokal) was applied to the data as both the MODIS Aqua chlorophyll retrievals and the *in situ* data are affected by measurement errors (Table 3). Even though the Spearman correlation coefficient was lower for ChL_LMI than for CHL_gsm, the slope regression coefficients for the LMI_CLU4 algorithm were close to the 1:1 line for the samples collected within 1 and 3 hours of the overpass while the gsm algorithm appeared to be overestimating the in situ data by a factor ~1.6. These results are consistent with the findings of the sensitivity analysis carried out for these coastal waters (Qin et al., 2007). The Bias for the MODIS Aqua chlorophyll retrievals by the LMI_CLU4 algorithm were nil but the percentage error was quite high (~110-120%).

The comparison of MODIS Aqua chlorophyll retrieval with *in situ* data showed that revised parameterization of regional algorithm coupled with the Artificial neural network atmospheric correction led to an improvement in accuracy since the previous report. In all likelihood further improvements possible within a year will enhance the confidence in the remote sensing estimates to the degree that remote sensing can become the prime detection and monitoring tool for chlorophyll, TSM and K_d estimates in the GBRWHA.

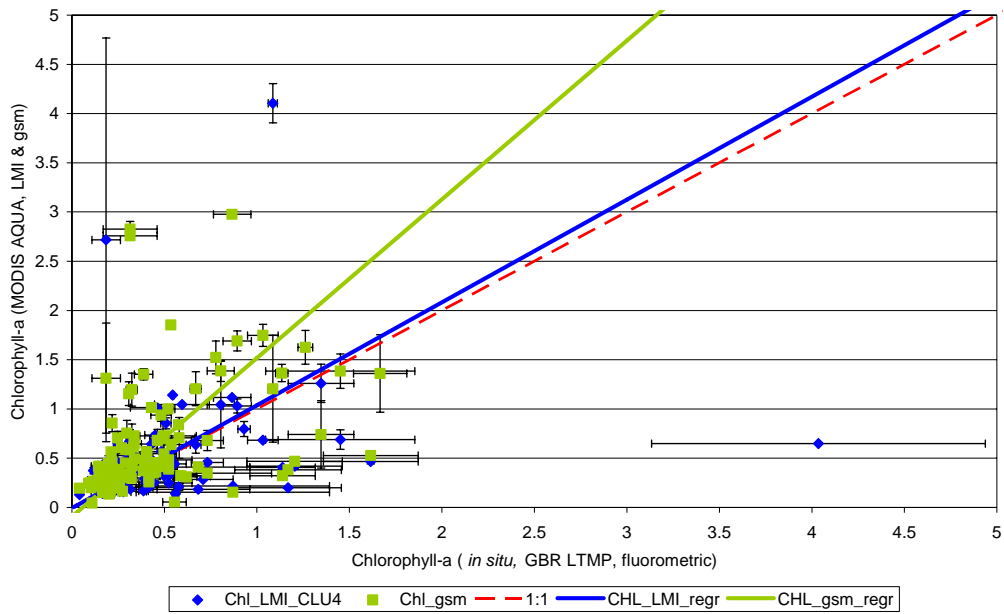


Figure 9: MODIS Aqua chlorophyll retrieval vs. in situ data. Only the measurements collected with 3 hours of the overpass were plotted. Number of matchups are 102 for LMI and 118 for gsm. The parameters for the regression lines are reported in Table 3.

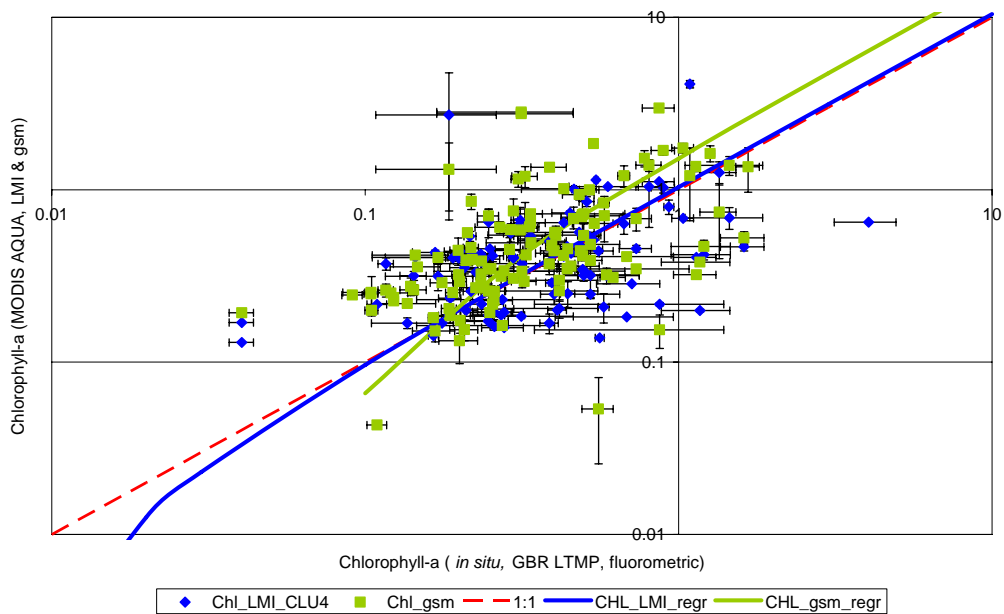


Figure 10: MODIS Aqua chlorophyll retrieval vs. *in situ* data. Same as Figure 9, but with log-log scale to enhance the range between 0.1 and 1 $\mu\text{g L}^{-1}$.

Table 3 Model II regression statistics for the measurements collected with 3 hours of the overpass. r is the Spearman correlation coefficient, RMSE the root mean square error

	hours	N	slope	Intercept	r	Bias	RMSE	%error
LMI	1	41	1.11	-0.04	0.13	0.01	0.42	119%
LMI	3	102	1.04	-0.01	0.24	0.01	0.48	107%
Gsm	1	49	1.54	-0.09	0.20	0.16	0.57	138%
Gsm	3	118	1.61	-0.10	0.42	0.17	0.49	111%

In this study, focus was on the chlorophyll estimations as that is the only suitable data available for validation. The MIM inversion method also simultaneously retrieves TSM and CDOM. Thus, these estimates are based on an internally consistent, physics-based description of light in water as a function of light absorption and light scattering by the three water quality variables.

To strengthen the validation of remote sensing data, the validation database should be extended to include water quality data sets used in recent studies on the spatial and temporal patterns of water quality of the Great Barrier Reef (De'ath 2007, 2008). The Secchi depth database would allow a direct validation the Secchi Depth estimates done from remote sensing data.

Our group is currently setting up the Lucinda Jetty Coastal Observatory (LJCO), as part of the Australian National Mooring Network, one the facilities of Australia's Integrated Marine Observing System (IMOS). LJCO aims to provide valuable data in tropical Queensland coastal waters to unravel the inaccuracies in remotely-sensed satellite ocean colour products due to the optical complexity in coastal waters and the overlying atmosphere. The LJCO data stream will increase the number of satellite vs. in situ match-ups assessment of normalized water-leaving radiances, water inherent optical properties and aerosol optical properties.

In the meanwhile, AIMS is leading the setup of GBROOS (Great Barrier Reef Ocean Observing System). Several autonomous water quality loggers will be deployed in GBR waters. In the future, the GBROOS data sets should also be used to evaluate and improve the accuracy of remote sensing retrieval.

Management relevant remote sensing products to monitor water quality in GBR

If environmental managers in the GBRWHA are to take full advantage of remote sensing capabilities then products that translate remotely-sensed scenes into useful information for managers are required.

The main needs of the end users of spatially explicit water quality data (see Table 4) can be summarised as:

- Status description and trend detection
- Characteristics of river plumes such as influence on high value assets, Observation of extent of influence of river plumes, definition of areas of Water Quality risk
- Compliance against targets: over spatial areas or specific assets, during river plumes, or risk hotspots
- Link monitoring & modelling – RS provides monitoring components. RS can be used to validate receiving water model with RS data.

To enable the adoption of remote sensing products in the adaptive management of GBR coastal waters it is imperative that these products are:

- suitable for use in media, web and report cards;
- presented in a manner that can be interpreted and used by managers (training and education loop between providers and users is needed);
- accompanied by a user guide for the range of products;

CSIRO’s Environmental Earth Observation Group developed a software suite to produce from daily remote sensed data a number of derived products suited to the specific needs of end-users, in a number of outputs, including maps, animations, statistical compliance assessments and alert or anomaly systems (see Table 4). The software suite enables the production of maps of:

- Min, Max, Median, Logmean, Mean, STD of Chlorophyll, TSM, CDOM and Kd for the GBRWHA.
- Maps of 5th, 25th, 75th and 95th of Chlorophyll, TSM, CDOM and Kd for the GBRWHA.
- Weekly, monthly, seasonal, and yearly and long term statistics
- Assessment of the nature of the exceedance of water quality guidelines for water quality variables

These products can also be used to

- Assess the relevance of current water compliance guidelines and creation of improved water quality compliance guidelines based on the actual behaviour of the coastal waters
- Analyse the correctness of hydrodynamic and biogeochemical models and subsequent improvement by data assimilation techniques.

In future, with the software suite, it will be possible to also produce:

- Trend analysis of Chlorophyll, TSM, CDOM and Kd over satellite sensor system life period
- Spatial and temporal autocorrelation analysis of Chlorophyll, TSM, CDOM and Kd.

All the maps and comparisons with in situ data presented in this report were produced using the above mentioned software suite. The software suite will be made available in the coming future to the GBRWHA management and research community. The methods for deriving management relevant products from remote sensing data will be contributed to the Reef Atlas to provide input into the GBRMPA Outlook report

Comment [bra372 2]: this text is new !

Table 4. Examples of potential application of remote sensing products addressing the main needs of the end users of spatially explicit water quality data

Need/Purpose	Audience/Users	Product
Status Trend Wet & dry seasons Characteristics of river plumes Influence on high value assets	NRM Managers Reef WQ Report State of Environment reporting	Regional - Mean concentrations in specified boundaries Ambient and event mapping
Observation of extent of influence of river plumes	NRM Managers General public	Satellite images showing extent of river plumes
Defining areas of WQ risk	NRM Managers General public	CDOM maps showing extent of terrestrial influence
Compliance against targets Spatial areas: Assets Plumes Risk hotspots	NRM Managers Reef Rescue mgt agencies	Within regions - Mean concentrations in specified boundaries
Target setting	NRM Managers Research projects eg. indicator development	Risk maps
Link monitoring & modelling – RS provides monitoring components. Use pilot in Fitzroy to validate receiving water model with RS data.	Managers -Target setting Research projects eg. developing receiving water models	Model parameterisation and validation

Results

The results for the six reporting regions are presented as wet and dry season median maps of chlorophyll (Figure 11), coloured dissolved organic matter (CDOM, Figure 12), total suspended matter (as non algal particulate matter, Figure 13) and the vertical attenuation coefficient of light (Figure 14). Also presented are maps for these dry and wet periods that present the number of valid pixels used for calculating the median values (Figure 16). Here we present only maps for the Fitzroy Estuary Keppel Bay region. The other regions (Cape York, Cairns, Burdekin, and Mackay-Whitsundays) are presented in the accompanying CD-ROM. All the maps and comparisons with in situ data presented in this report were produced using the above mentioned software suite.

Guide to interpreting the maps

All maps produce have a similar template: land is presented as dark grey, the coastal boundary is based on a standard coastline vector. Main rivers are presented in blue lines. Coral reefs including a 1 km buffer zone (to avoid mixed land or reef and water pixels) are presented as white.

Three lines are overlaid to the maps to enable the identification of water bodies consistently with the zones identified by De'ath (2007, 2008) to describe the spatial and temporal patterns of water quality of the Great Barrier Reef. The thick pink line is loosely based on the 20 m bathymetry line and defines the coastal waters; the thick grey line defines the outer boundary of the GBR lagoon, i.e. separates the inshore waters from the offshore waters; the thick black lines to the East in all images is the limit of the GBRWHA. These lines were loosely based on a bathymetry layer and on the reef mask as described in detail in the previous MMP report (Section 4, page 134, Schaffelke et al., 2006). Even though these lines do not exactly match the water body delineation proposed by De'ath (2007, 2008), they enable a comparison of the statistics of all the valid pixels per season per region, subdivided into inshore and offshore regions.

The final information in the maps are the long term monitoring stations, presented as pink numbers. The images show that many of these stations are situated very near to islands or coral reefs, rendering them less suitable for remote sensing product validation as all international remote sensing product validation protocols stipulate that validation match-ups will only be accepted if they are at least 5 km away from the nearest exposed land mass or submerged but still visible substratum.

The wet and dry season median maps for chlorophyll, suspended matter and vertical attenuation coefficient of light.

The wet and dry season median maps of chlorophyll (Figure 11) for the Fitzroy Estuary –Keppel Bay region show high chlorophyll levels near the coast and in the estuary to lower concentrations towards the East. Median values of Chlorophyll-a to $0.5 \mu\text{gL}^{-1}$ extended as far as the Bunker group for both seasons.

The wet and dry season median maps of coloured dissolved organic matter (CDOM, Figure 12) for the Fitzroy Estuary –Keppel Bay region show values higher than 0.20 m^{-1} in for a costal band ~10 km wide, up to 50 km north of the river mouth for the wet season, while during the dry season values were higher than 0.20 m^{-1} only for the area close to the river mouth.

The wet and dry season median maps of non-algal particulate matter (as a measure of total suspended matter) (Figure 13) for the Fitzroy Estuary –Keppel Bay region show similar gross patterns as for the CDOM distribution, although locally there are differences such as in towards the northeast of Shoalwater Bay where increased levels of non-algal particulate matter reach out further into the lagoon.

The wet and dry season median maps of vertical attenuation of light (Figure 14) for the Fitzroy Estuary –Keppel Bay region show similar gross patterns as for the chlorophyll, coloured dissolved organic matter and non-algal particulate matter distribution. The difference in dark blue to light blue colours between the wet and dry season for K_d is due to the K_d being slightly dependent on average

sun-angles during the satellite overpass- the reason is that sun light coming in at higher slant angles during the winter months is scattered more in the first meters of the water column. Care must be taken in interpreting the Shoalwater Bay results as we did not parameterise these waters for the bio-optical model (and they are presumably very different from our previously sampled waters) and there may be a bottom visibility issue too.

The wet and dry season median maps of water clarity expressed as Secchi depth (Figure 15) for the Fitzroy Estuary –Keppel Bay region show similar gross patterns to the maps of vertical attenuation of light (Figure 14). This product is still in development phase and should be validated using the water quality data sets used in recent studies on the spatial and temporal patterns of water quality of the Great Barrier Reef (De'ath 2007, 2008).

The maps in Figure 16 depict the number of image pixels per pixel location available for calculating the median values for each season. The maps show that this amount varies from 30 to about 90 for each season for each pixel location. Theoretically about 180 images should be available for each season. For the data of Dry Season 2007 and Wet Season 2007/2008 there were 150-170 images available. The reason for the significantly less available pixels is the quality control criteria we applied: pixels with cloud or cloud shadow were flagged and dismissed; pixels where the atmospheric correction failed were dismissed too: this caused the dearth of pixels in the very near coastal areas. Also dismissed were the pixels where the error between modelled and measured spectra was too high.

The number of image pixels per pixel location available for calculating the median values for each season increased from 5 to 60 of the previous MMP report to from 30 to about 90 of this study. This reduction of pixels being dismissed because of atmospheric correction failure or because the error between modelled and measured spectra was too high is a direct result of the implementation of the Artificial neural network atmospheric correction.

This is a good moment to remember that these results are for the MODIS Aqua sensor data only with its nominal 13:30 overpass time. The other MODIS sensor on board of Terra has been operational since 2000 and comes over at 10:00 in the morning when cloud cover is less. We chose to work with Aqua data first as the sensor is better characterised and therefore it was the most suitable for us to begin with. If we were to incorporate MODIS Terra data and were to improve the atmospheric correction over near coastal muddy waters the amount of pixels per wet or dry season could increase to over 120 per season, more likely up to 200 per season.

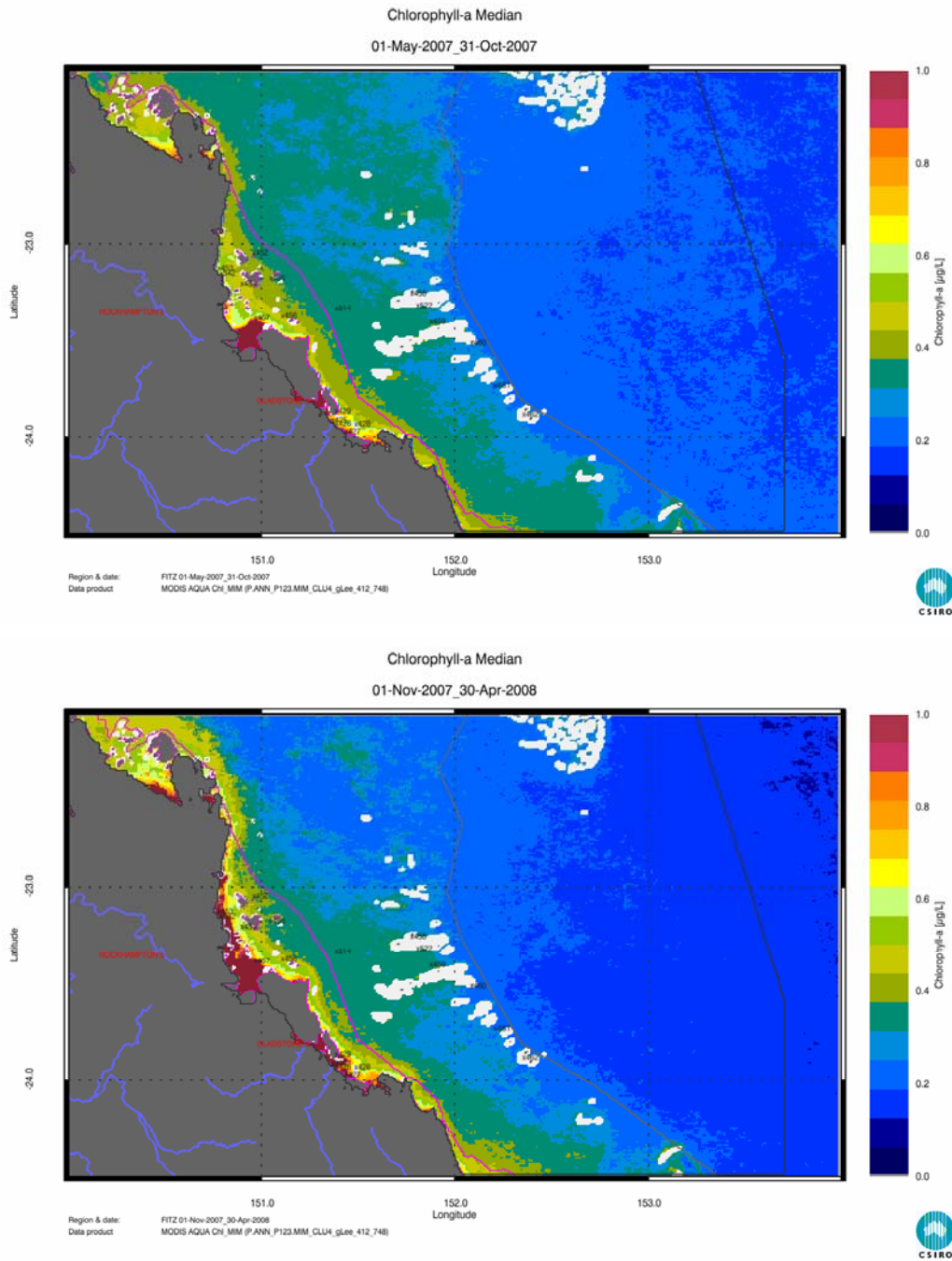


Figure 11. Chlorophyll Median maps for the dry and wet season for the Fitzroy Estuary –Keppel Bay region. Map a) (top panel) presents the median for the Dry Season 2007 (May - October), while map b) (bottom panel) presents the median for the Wet Season 2007/2008 (November 2007- April 2008). See text for annotation explanation.

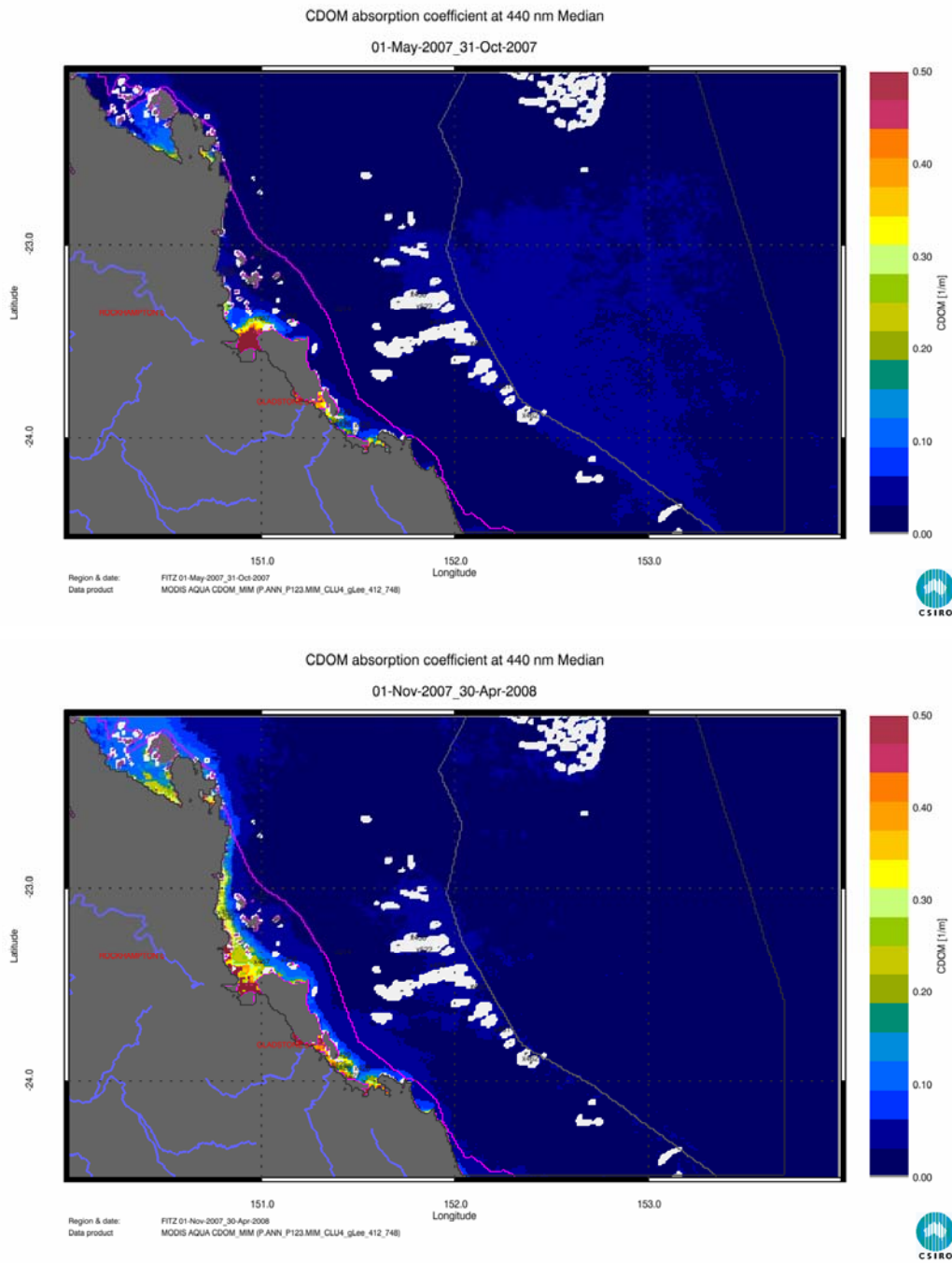


Figure 12. CDOM Median maps for the dry and wet season for the Fitzroy Estuary –Keppel Bay region. Map a) (top panel) presents the median for the Dry Season 2007 (May - October), while map b) (bottom panel) presents the median for the Wet Season 2007/2008 (November 2007- April 2008). See text for annotation explanation.

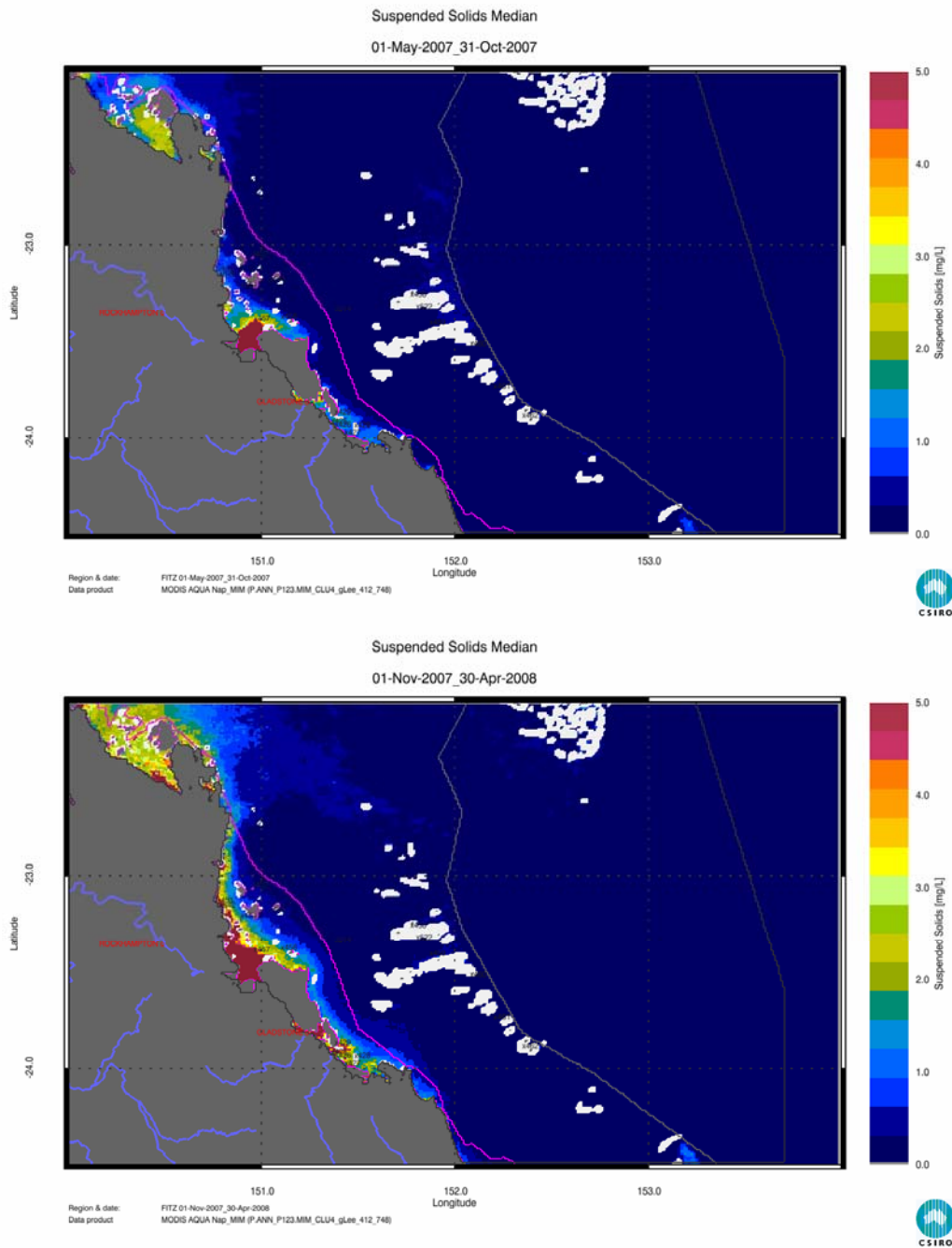


Figure 13. Non-algal particulate matter (Nap as a measure of TSM) Median maps for the dry and wet season for the Fitzroy Estuary –Keppel Bay region. Map a) (top panel) presents the median for the Dry Season 2007 (May - October), while map b) (bottom panel) presents the median for the Wet Season 2007/2008 (November 2007- April 2008). See text for annotation explanation.

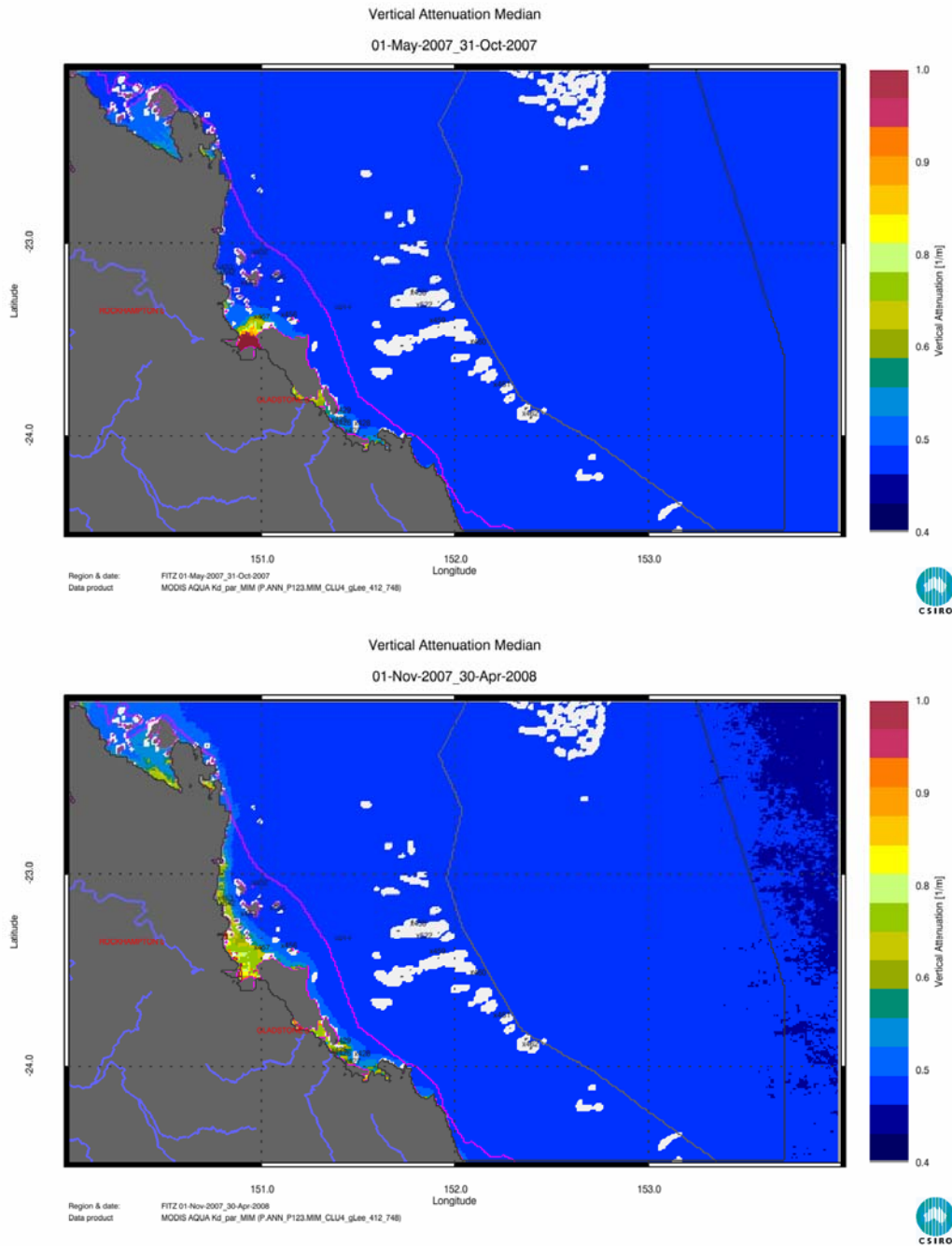


Figure 14. Vertical attenuation of light (K_d , as estimate of water clarity) Median maps for the dry and wet season for the Fitzroy Estuary –Keppel Bay region. Map a) (top panel) presents the median for the Dry Season 2007 (May - October), while map b) (bottom panel) presents the median for the Wet Season 2007/2008 (November 2007- April 2008). See text for annotation explanation.

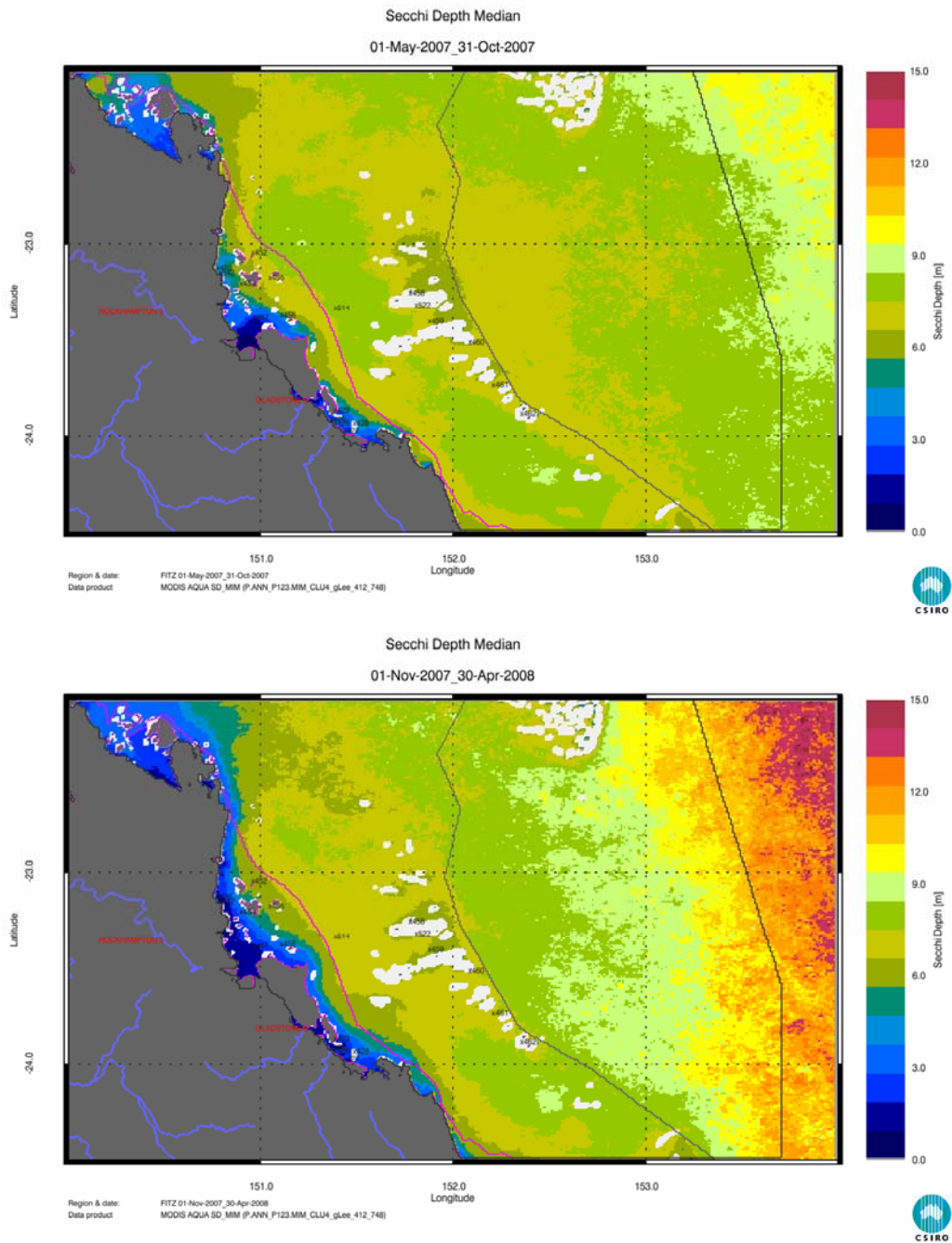


Figure 15. Secchi Depth (as estimate of water clarity) Median maps for the dry and wet season for the Fitzroy Estuary –Keppel Bay region. Map a) (top panel) presents the median for the Dry Season 2007 (May - October), while map b) (bottom panel) presents the median for the Wet Season 2007/2008 (November 2007- April 2008). See text for annotation explanation.

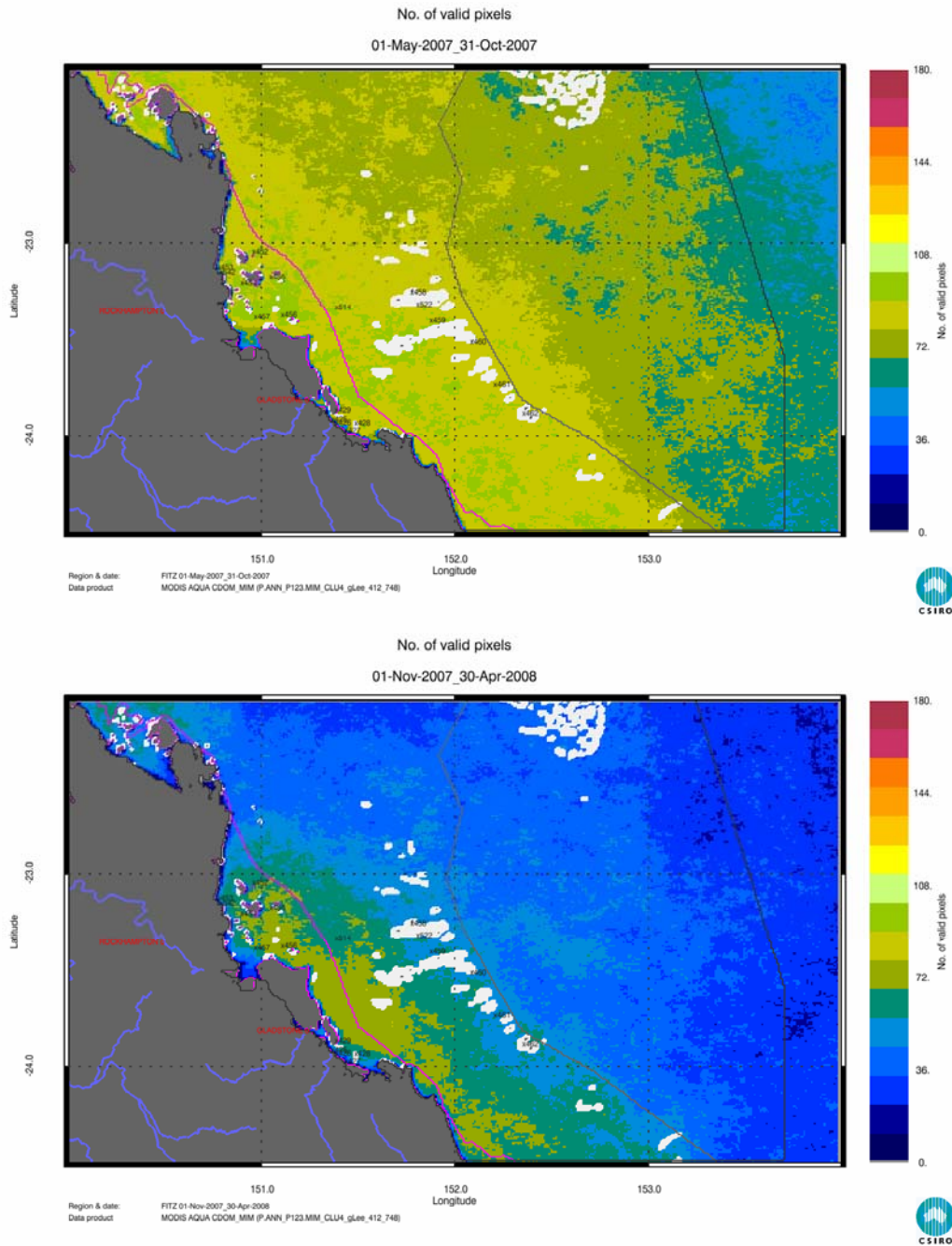


Figure 16. Number of pixels used to calculate the Median maps (Figure 11 - Figure 15) for the dry and wet season for the Fitzroy Estuary –Keppel Bay region (). Map a) (top panel) presents the number of pixels available for the Dry Season 2007 (May - October), while map b) (bottom panel) presents the number of pixels available for the Wet Season 2007/2008 (November 2007- April 2008). See text for annotation explanation.

Comparison of the in situ data distributions of the long term monitoring plan with the remote sensing data distributions

A comparison of the statistical distributions of the chlorophyll *a* from the in-situ data from the GBR LTMP and retrieved with the algorithm from MODIS-AQUA data is presented as box-whiskers plots for each region (Figure 17 through to Figure 21) for the wet and dry season 2005/2006. In each figure, the box-whiskers plots are organised in three panels: in-situ data from the GBR LTMP; satellite-derived, time-series data of the pixel encompassing the locations of GBR LTMP in situ sites; and all satellite-derived, time-series data. The box-whiskers plots for coastal, inshore and offshore regions are presented in each panel. These three areas were defined using the three lines that are overlaid to the maps to enable the identification of water bodies, as described previously.

For each season, area and year, the data used to calculate the distribution varies significantly; the in-situ samples from the LTMP comprise 10-50 data-points (sometimes as low as 5), the satellite imagery time series at the locations of the in-situ samples contain ~100-500 pixels, and the satellite imagery of the entire region varies from 75,000 to >500,000 pixels. The sampling frequency of the GBR LTMP data varied from monthly (for few coastal or inshore sites) to once or twice per season (mostly for the offshore sites). The satellite-derived, time-series data was extracted at all the available locations of GBR LTMP sites, even if any of these sites were not actually used for sampling in that season.

Sometimes one or more of the box-whiskers plots is missing from the figures for the in situ data or the satellite imagery time series at the locations of the in-situ samples. For the in situ data the distributions were calculated if at least five data points were available, while sometime none of GBR LTMP sites were in locations not masked by the reef or land mask in the satellite imagery for a given region (coastal, inshore or offshore). Details of these occurrences are reported in the legends of each figure.

Because the in situ sampling locations are by definition not randomly distributed and the remote sensing images samples completely on clear days (full sampling), to partially (but quite random sampling) on partially cloudy days to not at all on overcast days statistically a direct comparison is not allowed.

In general the box-whiskers plots show higher chlorophyll value expressed as medians and 25 to 75% percentiles for the in situ samples and the remote sensing estimates of the waters in the coastal region than for the waters in inshore region and the offshore region. Most of the times the ranges of the measured in situ samples fall within the ranges of the remotely sensed values. This makes sense as the remote sensing data is based on (sometimes) full coverage of all the water body over the coastal, inshore or offshore regions. However the medians and 25 to 75 % percentiles do differ. For the offshore regions in all of the figures this most likely due to an under representation of oceanic water sites as the sampling station locations of the in situ data that are often close to reefs. The remote sensing data contains much more oceanic water type pixels than the in situ sampling stations do. A similar effect is likely to occur also for the inshore waters

The box-whiskers plots presented here show that in situ measurements are limited in scope and coverage of all actual concentration ranges occurring everywhere. In essence in situ programmes deliver 10 to a hundred spot samples in one of these regions whereas this first satellite dataset already delivers hundreds of thousands of measurements of 1 square kilometre covering virtually all occurring concentration range and events.

To provide further information on the spatial variability of water quality in the GBR waters the deployment of automated measuring systems on "Ships of Opportunity" should be considered. Ships should be fitted with automated sensors which record the water quality parameters such as temperature, salinity, turbidity, oxygen, nutrients and chlorophyll during the trip. Such systems are already used for operational observations of water quality in different regions of the world.

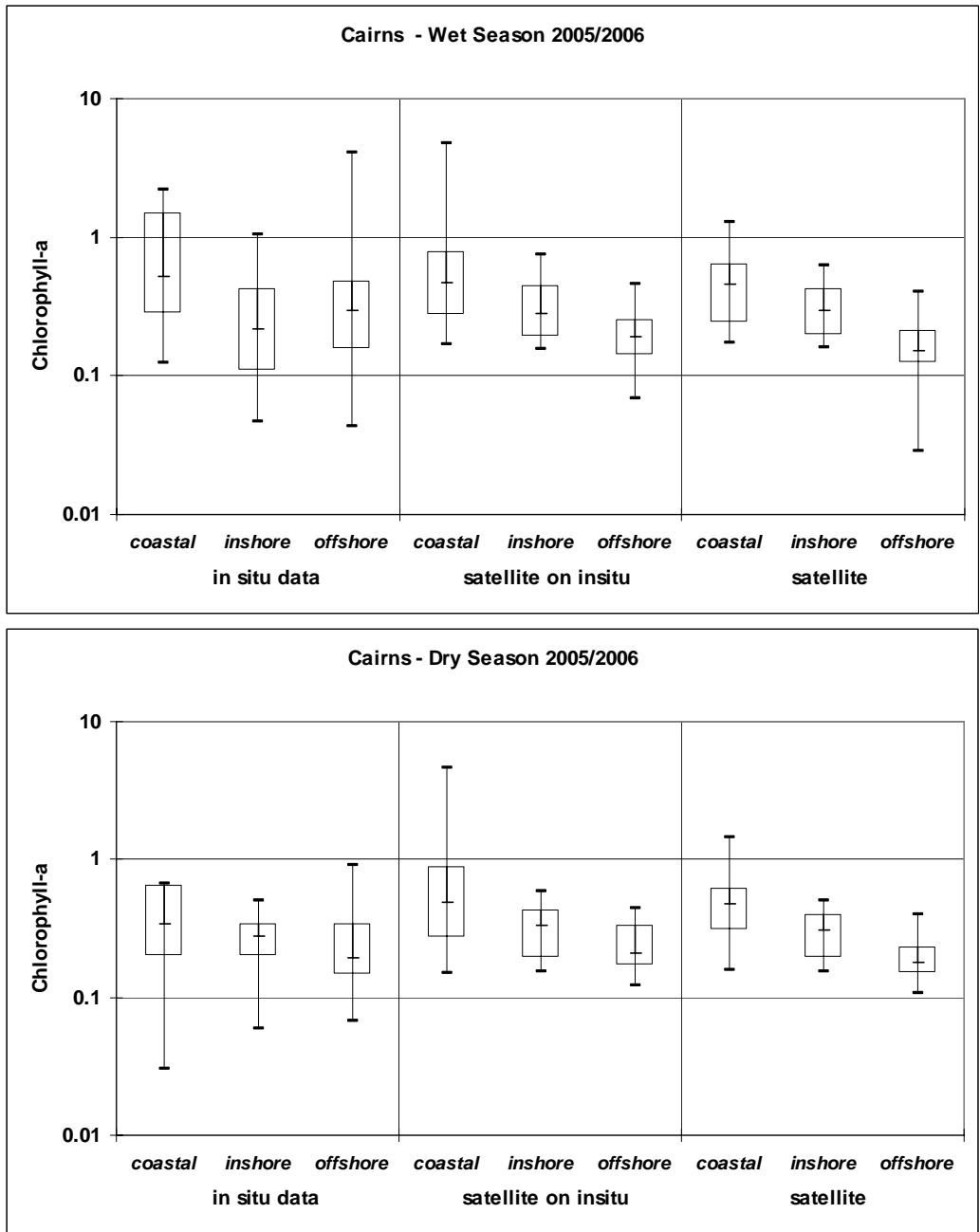


Figure 17. Comparison of chlorophyll concentrations retrieved from MODIS-AQUA data with in-situ data from the GBR LTMP for the CAIRNS region. Figures a and b results for dry and wet season of 2005/2006. The nine box-whiskers plots are organised in three panels: in-situ data from the GBR LTMP; satellite-derived, time-series data of the pixel encompassing the in situ sites; and all satellite-derived, time-series data. The box-whiskers plots for coastal, inshore and offshore regions are presented in each panel.

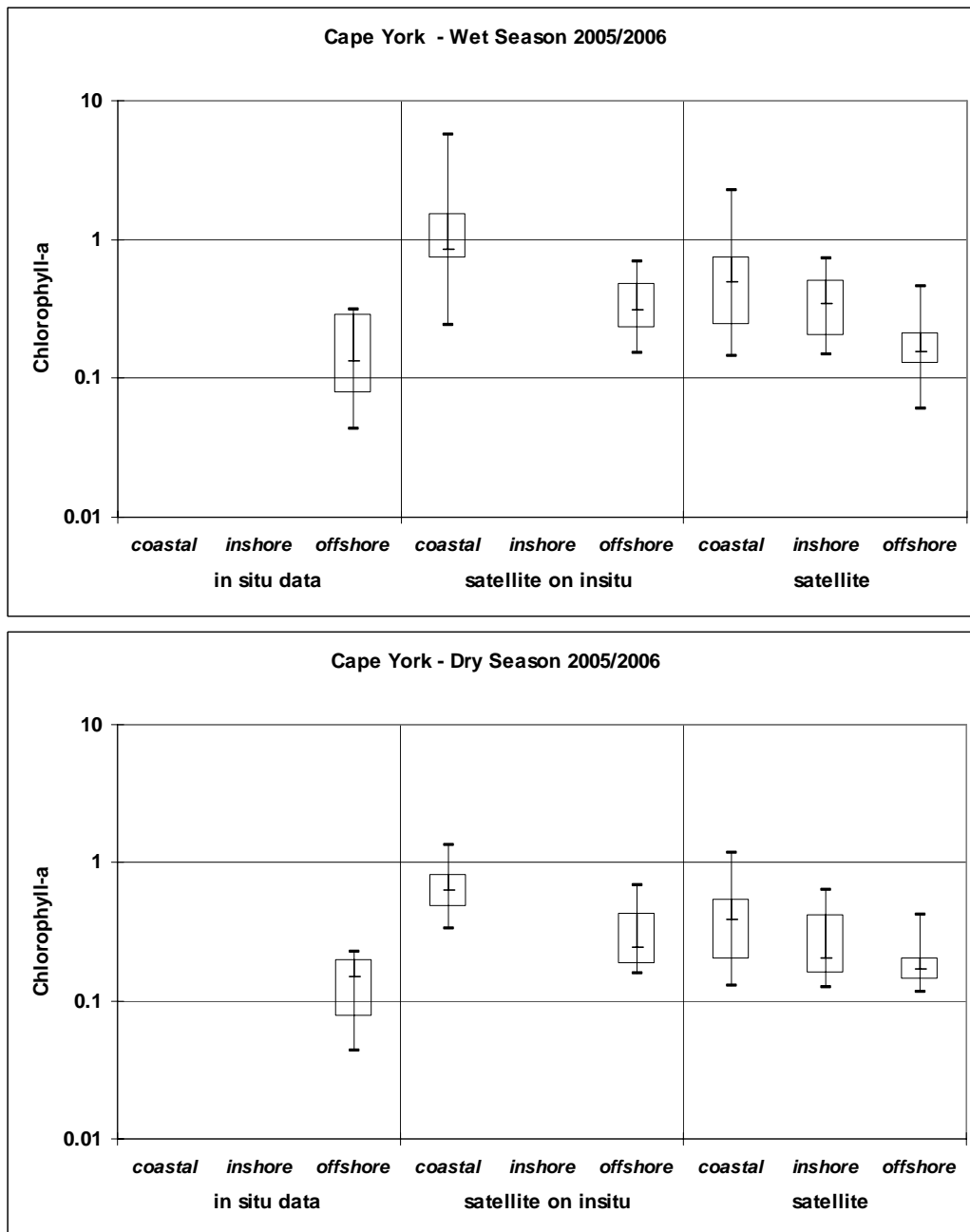


Figure 18. Comparison of chlorophyll concentrations retrieved from MODIS-AQUA data with in-situ data from the GBR LTMP for the Cape York region. Figures a and b results for dry and wet season of 2005/2006. The nine box-whiskers plots are organised in three panels: in-situ data from the GBR LTMP; satellite-derived, time-series data of the pixel encompassing the in situ sites; and all satellite-derived, time-series data. The box-whiskers plots for coastal, inshore and offshore regions are presented in each panel. Of the GBR LTM sites, site 483 was visited in the coastal region, and sites 489, 492, 493, 495, 511, and 521 in the offshore region, site 483 was visited only twice and the box-whiskers plot was not reported. Only sites 483, 489, 493, and 494 were in locations not masked by the reef or land mask in the satellite imagery.

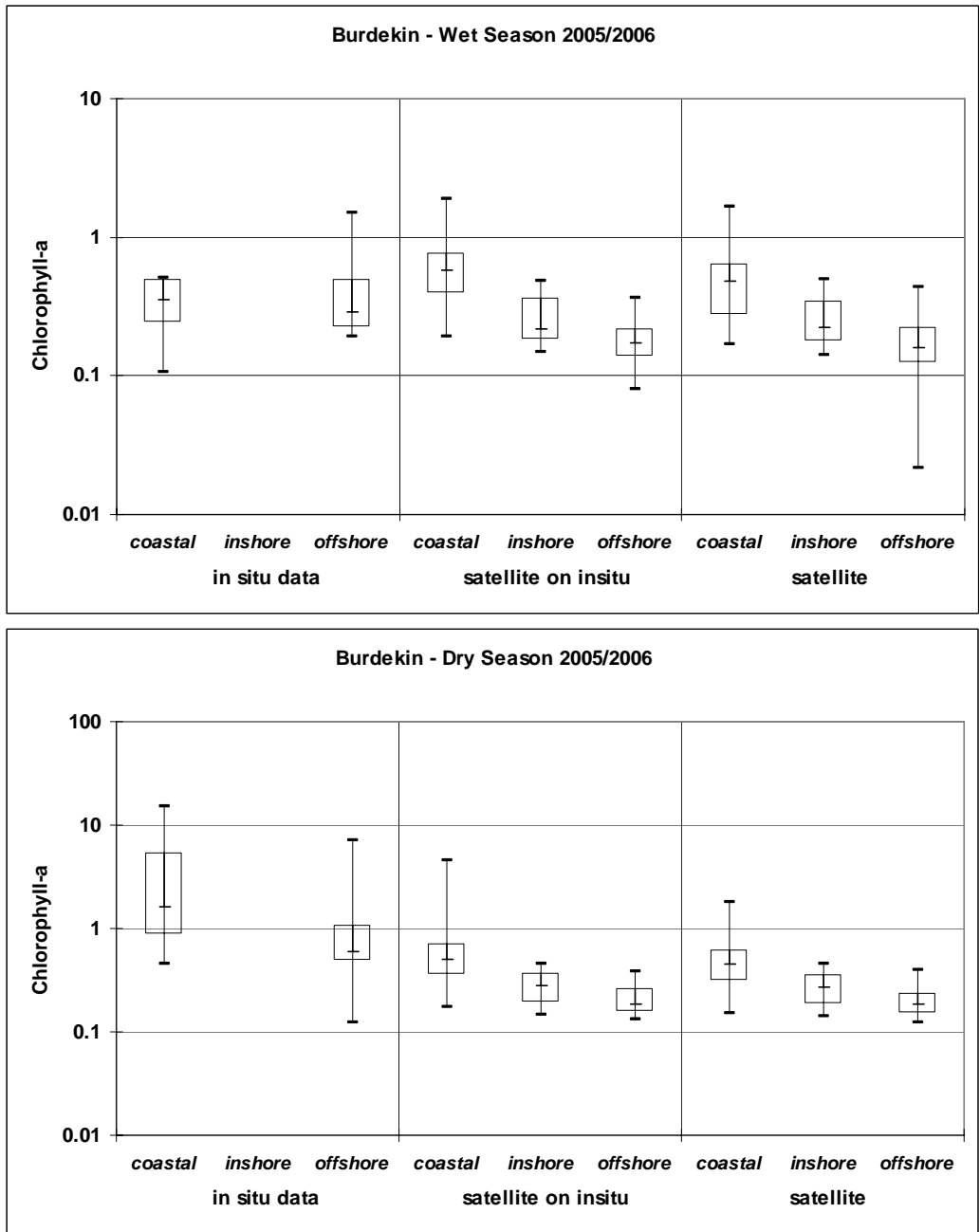


Figure 19. Comparison of chlorophyll concentrations retrieved from MODIS-AQUA data with in-situ data from the GBR LTMP for the Burdekin region. Figures a and b results for dry and wet season of 2005/2006. The nine box-whiskers plots are organised in three panels: in-situ data from the GBR LTMP; satellite-derived, time-series data of the pixel encompassing the in situ sites; and all satellite-derived, time-series data. The box-whiskers plots for coastal, inshore and offshore regions are presented in each panel. Of the GBR LTM sites, site 523 was visited only twice in the inshore region and the box-whiskers plot was not reported.

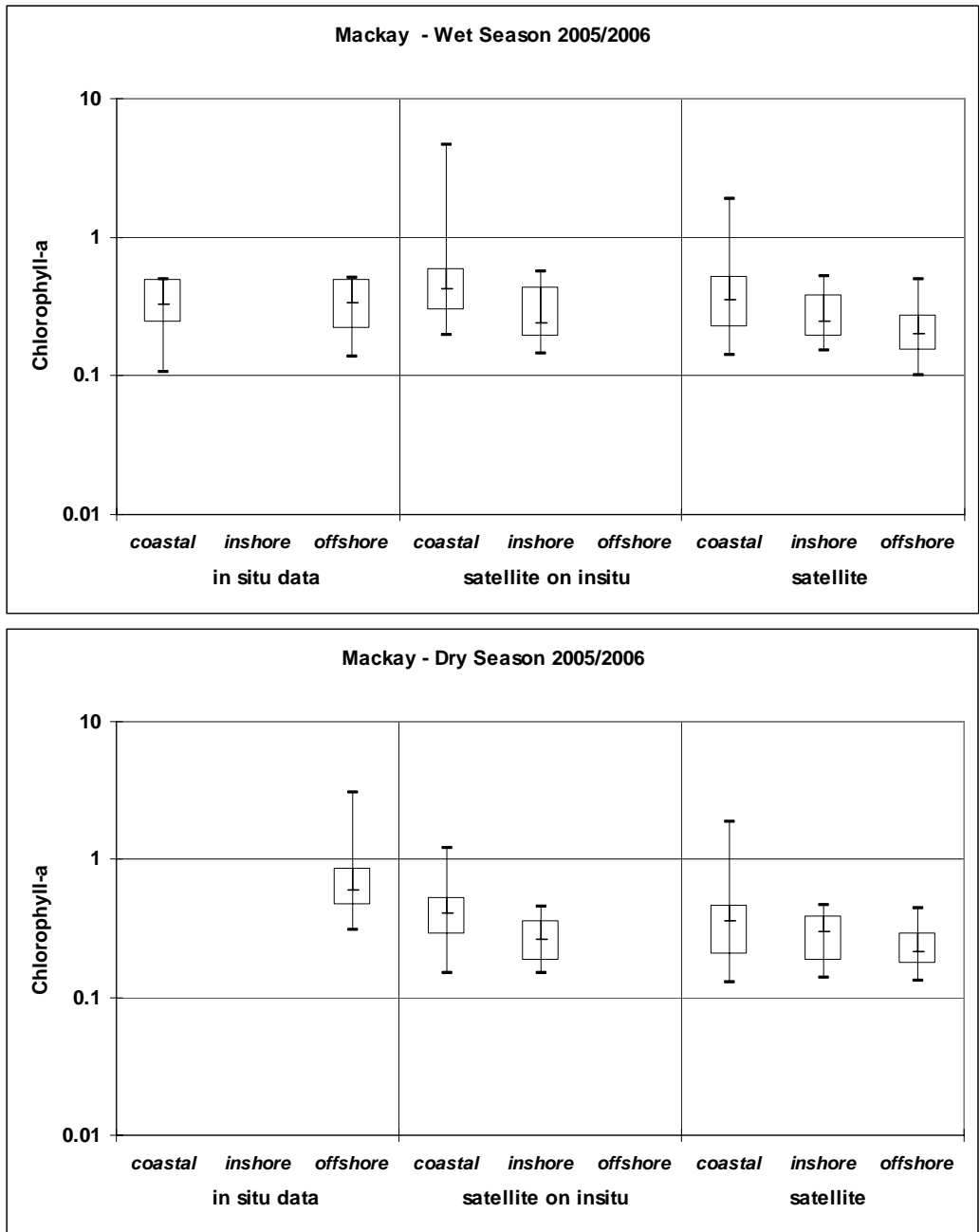


Figure 20. Comparison of chlorophyll concentrations retrieved from MODIS-AQUA data with in-situ data from the GBR LTMP for the Mackay region. Figures a and b results for dry and wet season of 2005/2006. The nine box-whiskers plots are organised in three panels: in-situ data from the GBR LTMP; satellite-derived, time-series data of the pixel encompassing the in situ sites; and all satellite-derived, time-series data. The box-whiskers plots for coastal, inshore and offshore regions are presented in each panel. Of the GBR LTM sites, sites 473 for the coastal region and 540, 541, 1444 in the offshore region were visited; site 473 was visited only twice during the dry season and the box-whiskers plot was not reported. Only sites 473, 474, 478, 479, 481 and 1445 were in locations not masked by the reef or land mask in the satellite imagery.

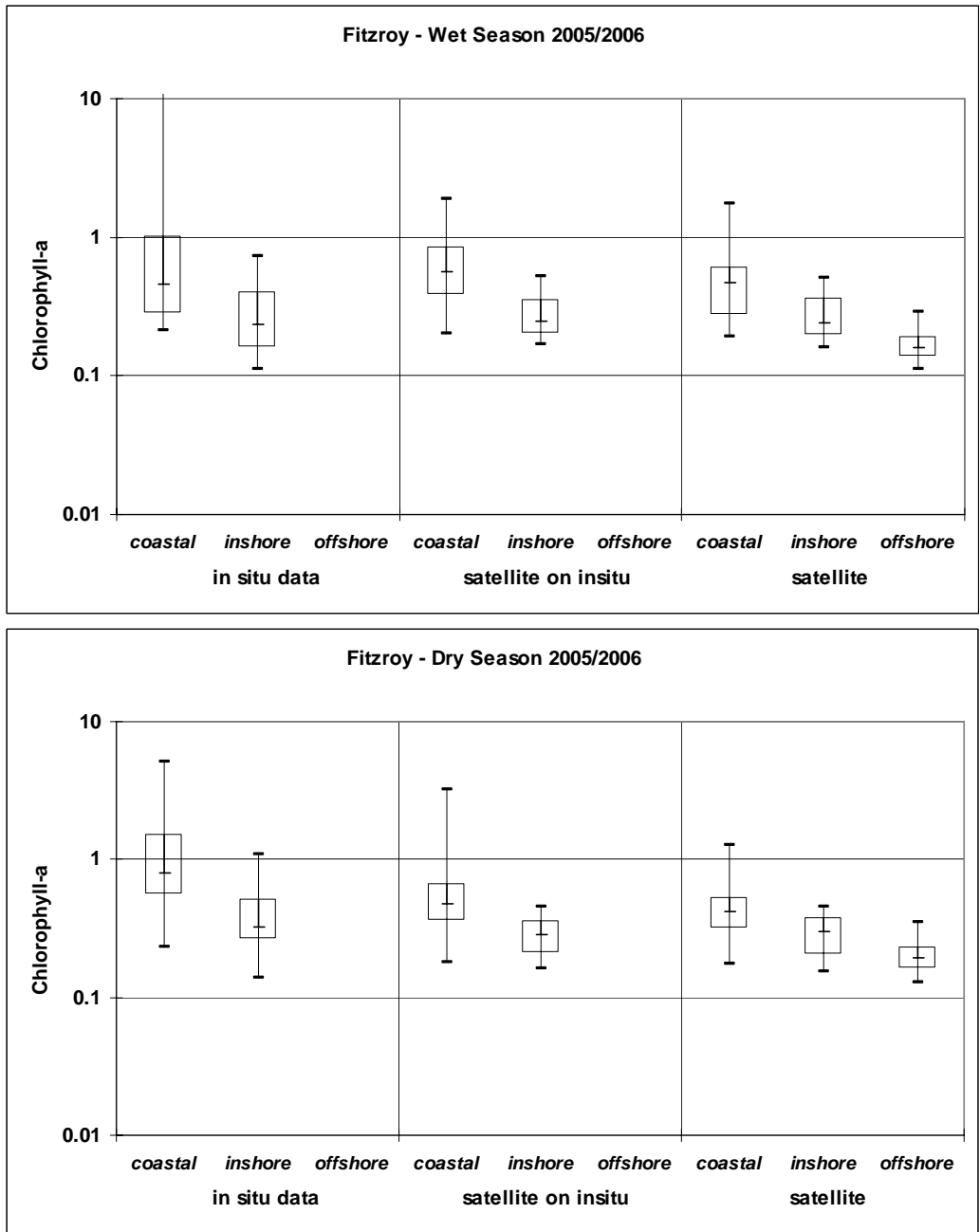


Figure 21. Comparison of chlorophyll concentrations retrieved from MODIS-AQUA data with in-situ data from the GBR LTMP for the Fitzroy region. Figures a and b results for dry and wet season of 2005/2006. The nine box-whiskers plots are organised in three panels: in-situ data from the GBR LTMP; satellite-derived, time-series data of the pixel encompassing the in situ sites; and all satellite-derived, time-series data. The box-whiskers plots for coastal, inshore and offshore regions are presented in each panel. None of GBRLTM sites were located within the offshore region.

Flood plume mapping

The extent and duration of flood plumes can have significant implications for the health of inshore marine ecosystems, such as seagrasses and coral reefs. The dynamics of a flood plume as it moves from the river mouth into the marine environment can be described in terms of the hydrological and chemical behaviour. At first flood plumes contain elevated concentrations of sediments (and associated nutrients and pesticides). Later, when particulate matter falls out of the plume waters the plume is characterised mainly by presence of the dissolved materials (and the associated nutrients).

The daily maps of CDOM and the maximum retrieved CDOM values for the wet season were made available to Michelle Devlin (ACTFR) to carry out further research in mapping extent and duration of the primary and secondary plumes within another MTSRF project.

To evaluate the overall effect of the flood event occurred in the Fitzroy River in January-February 2008, the Median maps for the Fitzroy Estuary –Keppel Bay region for the Wet Season 2007/2008 (November 2007- April 2008, Figure 11a - Figure 16a) should be compared with Median maps for the wet season 2006/2007 when no flow event occurred (November 2006- April 2007, Figure 22 -Figure 25).

All variables showed a larger extent of the coastal influence in 2008, when the flood event occurred. Median values of Chlorophyll-a of $\sim 0.5 \mu\text{gL}^{-1}$ extended as far as the Bunker group. CDOM Median values were almost double in Keppel Bay: in 2008 CDOM median was higher than 0.20 m^{-1} in a costal band $\sim 10 \text{ km}$ wide, up to 50 km north of the river mouth. NAP Median values were similar for the two seasons, but differences can be seen when comparing the 75th and 95th percentiles maps (figures not shown).

The extent of the river plume in 2008 is presented for key dates to characterize the late January and mid February peak events as the pseudo true colour composites and the daily CDOM maps (Figure 26). The first image, 28th January, shows the primary plume constrained to the coast and within a small salinity zone. The secondary plume moves northwards, still relatively close to the coast. The high CDOM concentrations retrieved from the 21st and 22nd February imagery show that the offshore influence of the Fitzroy flood was more significant in the second flow event, possibly due to the very high volumes of flow from the second event. Also the cloud cover in days following the first flow event hindered the satellite imagery acquisition during the secondary plume phase. By the 8th March, the CDOM signal was once again constrained to the shore and measured only north of the river mouth.

The extent of the river plume in 2008 can be characterized in detail by comparing the maps of the 75th and 95th percentiles and the maximum retrieved CDOM values of the 2007/2008 wet season to the previous year when no flow event occurred. (Figure 27 - Figure 29). The 75th percentiles map for 2008 (Figure 27b) shows values higher than 0.50 m^{-1} for the costal band $\sim 10 \text{ km}$ wide, up to 50 km north of the river mouth, for which values of 0.30 m^{-1} were observed in 2007(Figure 27a). The values of CDOM in the 75th percentiles map for 2008 are comparable in magnitude with the 95th percentiles of the 2007 wet season (Figure 28a).

The map of the maximum retrieved CDOM values for 2008 (Figure 29a) clearly shows the lobes of high concentrations of dissolved materials that were observed from the daily imagery (Figure 26) and in the field during the late January and mid February peak events. Values higher than 0.50 m^{-1} were observed in Keppel bay for a radius of 40 km from the river mouth and in a costal band $\sim 20 \text{ km}$ wide, up to 50 km north of the river mouth.

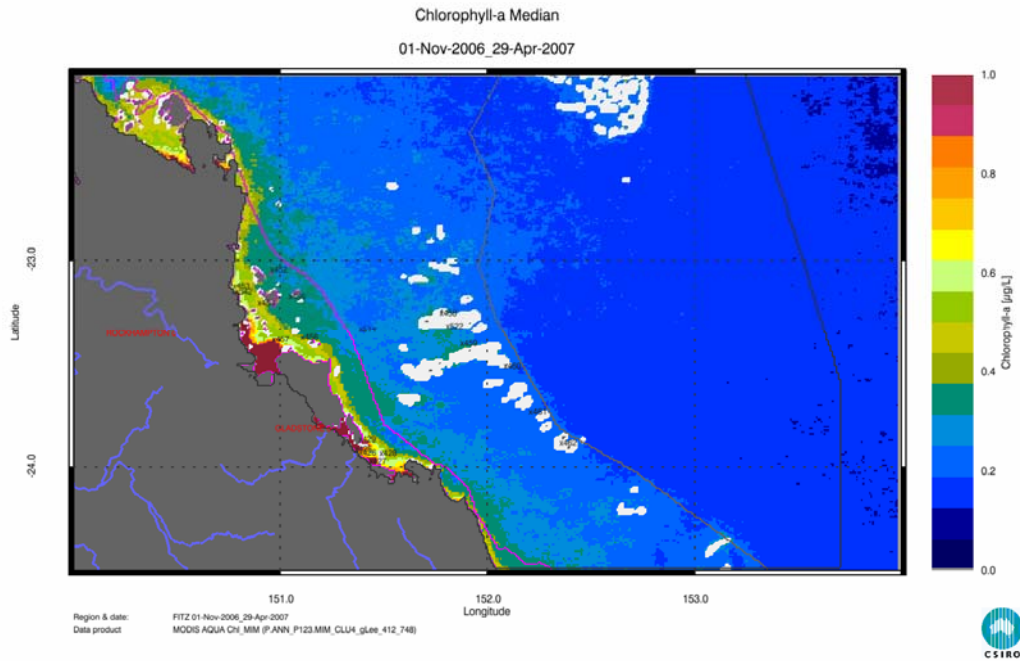


Figure 22. Chlorophyll Median maps for the wet season 2006/2007 (November 2006- April 2007) for the Fitzroy Estuary –Keppel Bay region. See text for annotation explanation.

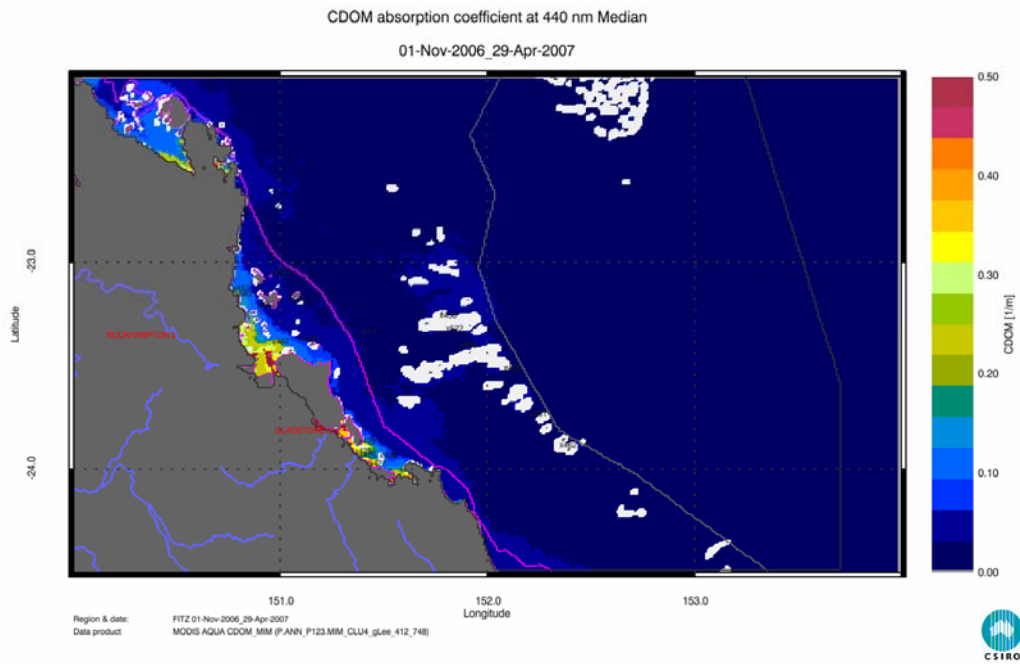


Figure 23. CDOM Median maps for the wet season 2006/2007 (November 2006- April 2007) for the Fitzroy Estuary –Keppel Bay region. See text for annotation explanation.

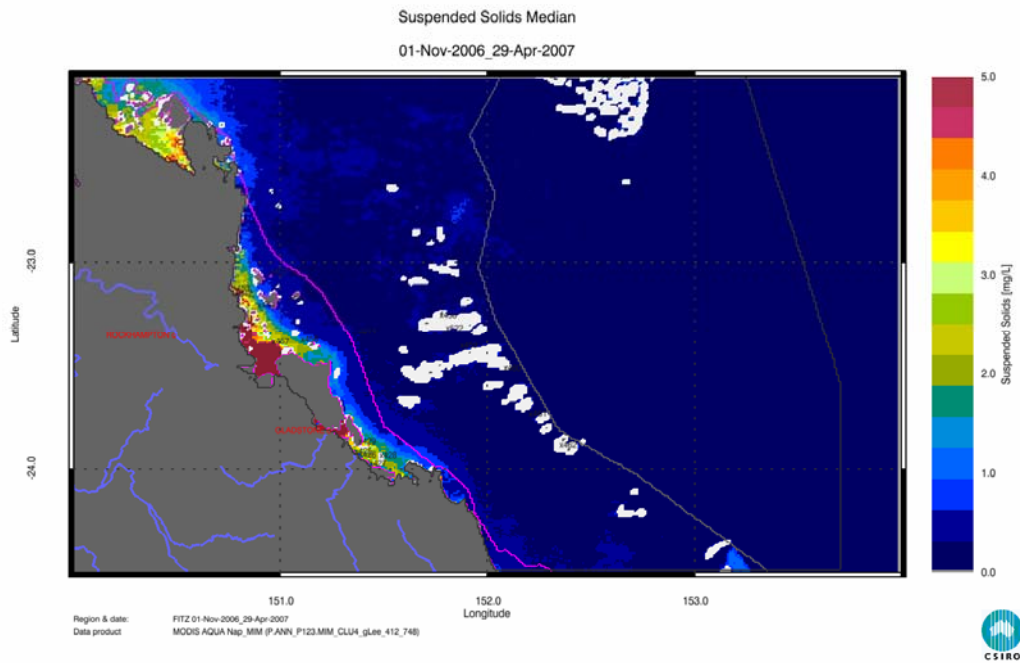


Figure 24. Non-algal particulate matter (Nap as a measure of TSM) Median maps for the wet season 2006/2007 (November 2006- April 2007) for the Fitzroy Estuary –Keppel Bay region. See text for annotation explanation.

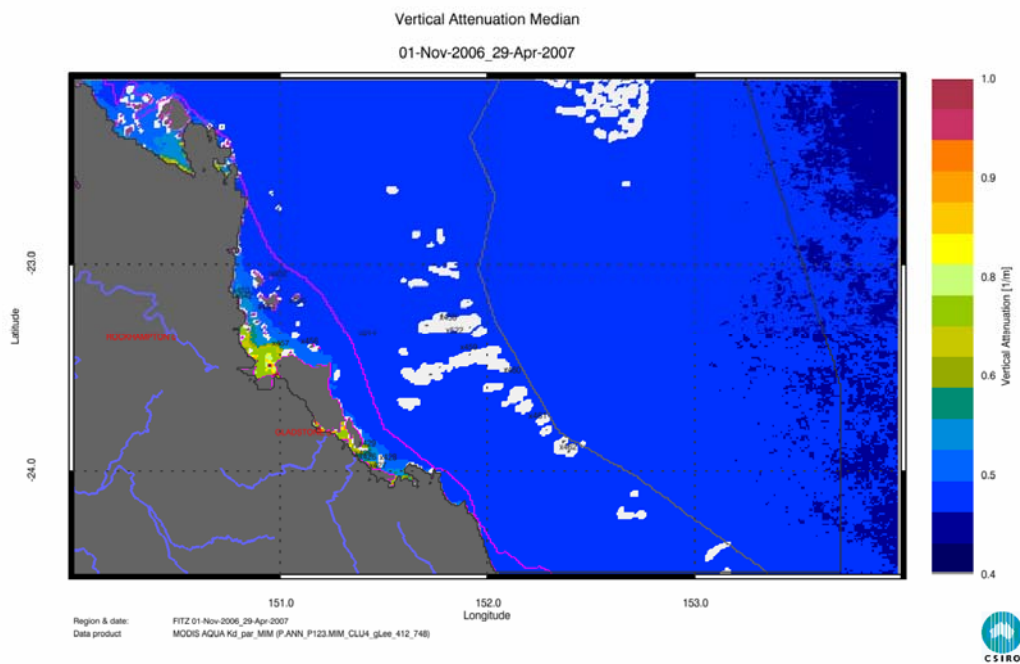


Figure 25. Vertical attenuation of light (K_d , as estimate of water clarity) Median map for the wet season 2006/2007 (November 2006- April 2007) for the Fitzroy Estuary –Keppel Bay region. See text for annotation explanation.

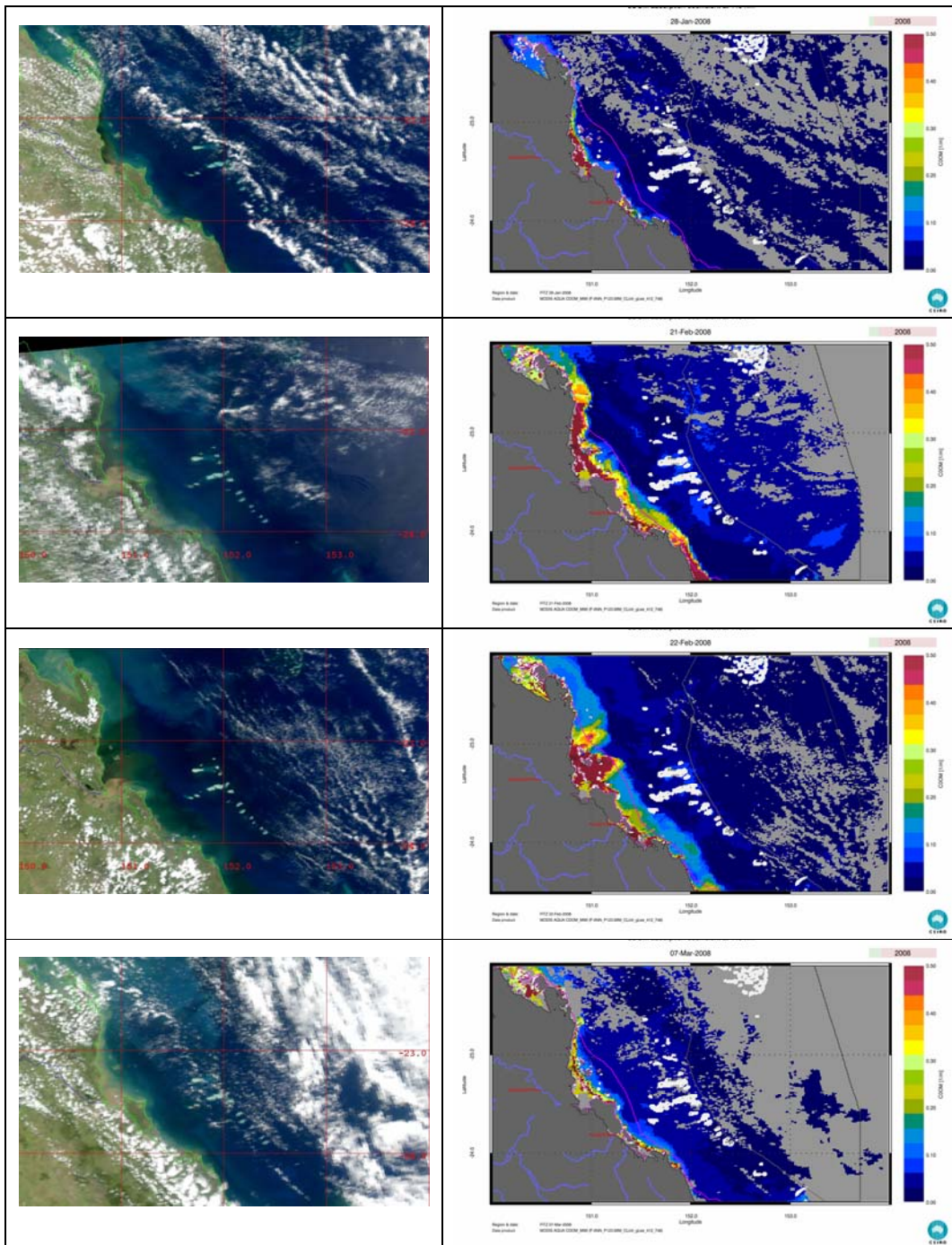


Figure 26. Daily true colour images and CDOM maps for key dates during the 2008 flood event for the Fitzroy Estuary –Keppel Bay region. From top to bottom: 28 January 2008, 21 February 2008, 22 February 2008 and 7 March 2008. See text for annotation explanation.

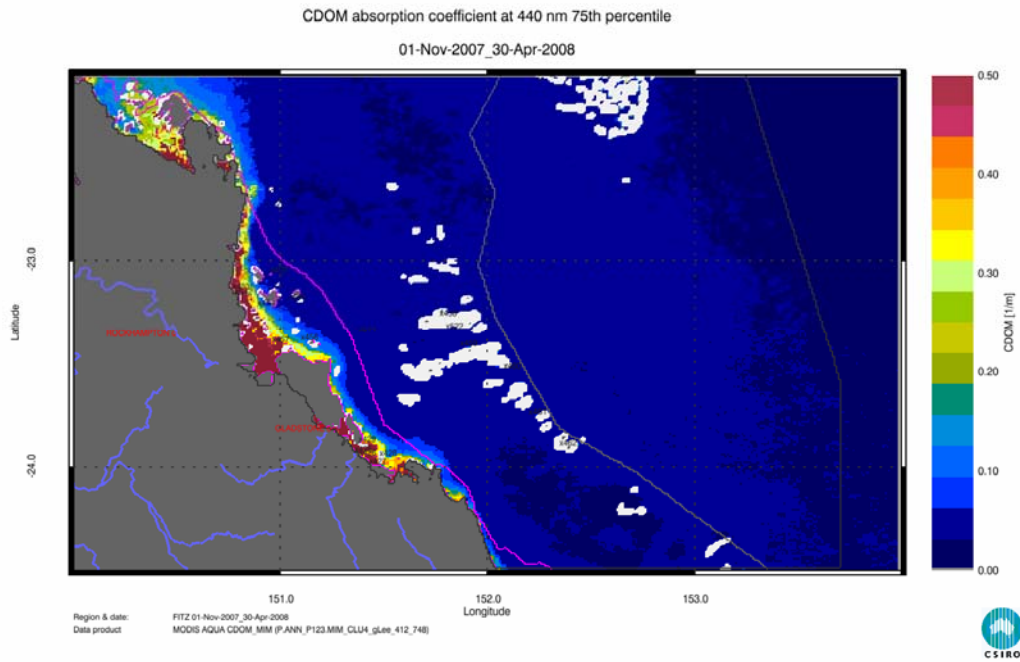
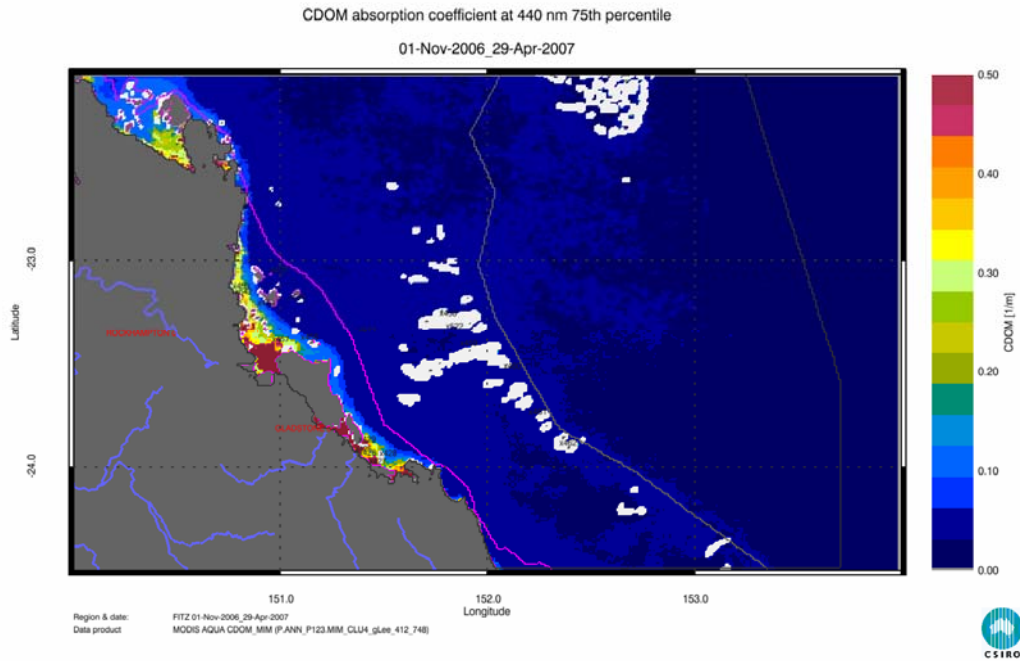


Figure 27. Maps of the 75th percentiles for CDOM for the wet season 2006/2007 and 2007/2008 for the Fitzroy Estuary –Keppel Bay region. See text for annotation explanation.

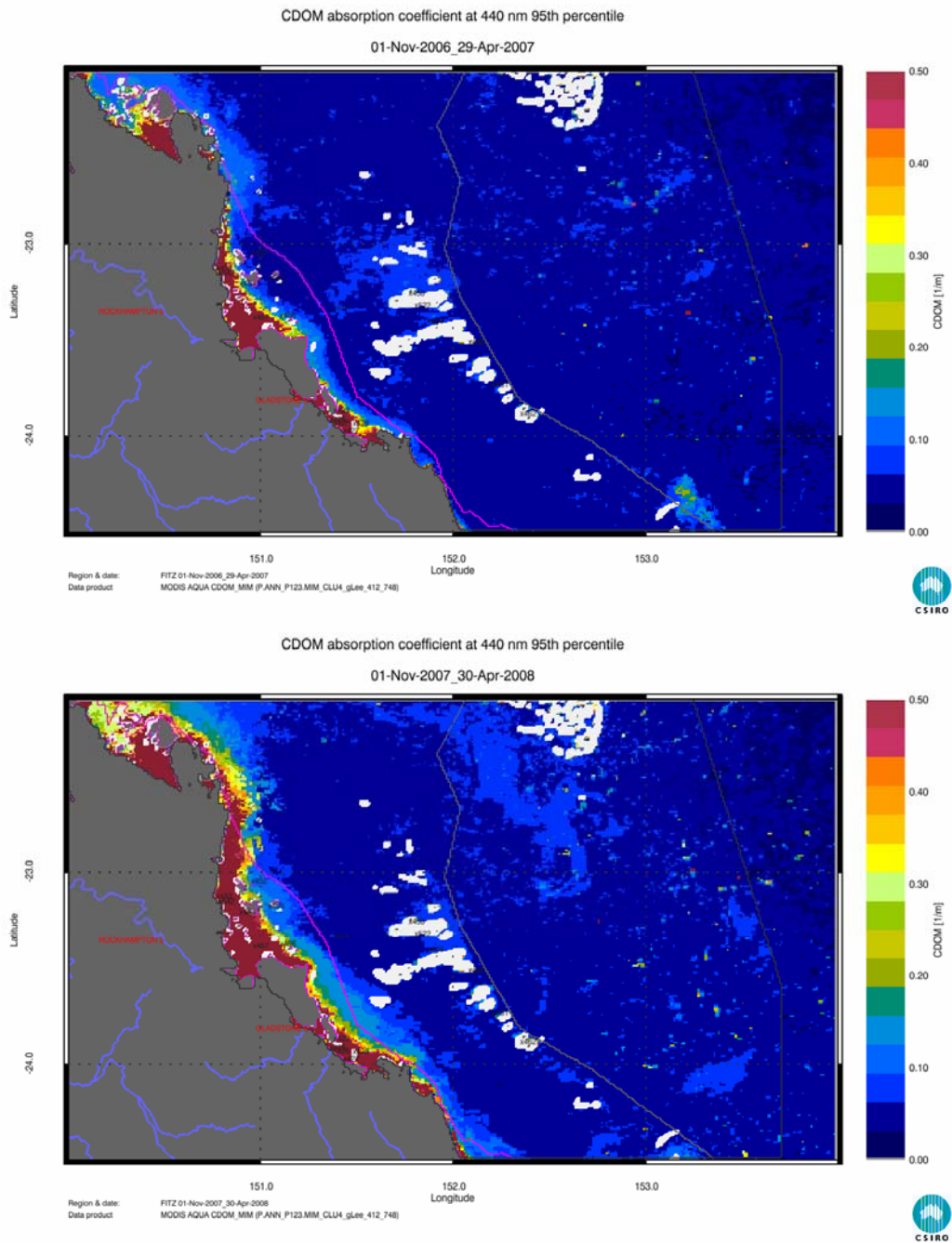


Figure 28. Maps of the 95th percentiles for CDOM for the wet season 2006/2007 and 2007/2008 for the Fitzroy Estuary –Keppel Bay region. See text for annotation explanation.

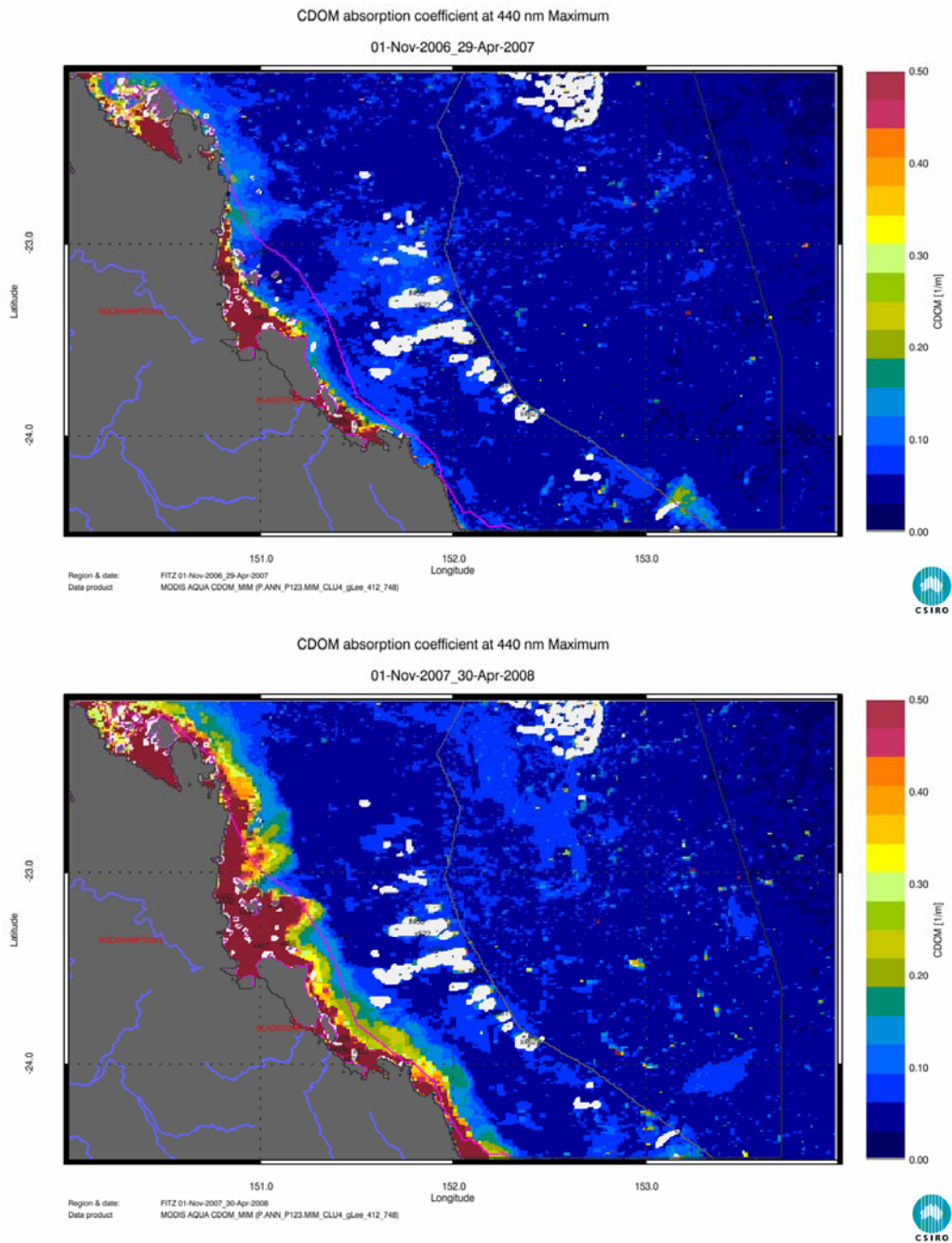


Figure 29. Maps of Maximum retrieved value of CDOM for the wet season 2006/2007 and 2007/2008 for the Fitzroy Estuary –Keppel Bay region. See text for annotation explanation.

ACKNOWLEDGMENTS

Lesley Clementson, for discussion on phytoplankton absorption spectra

APPENDIX B NOTES ON DETECTING TRICHODESMIUM SP. IN MERIS IMAGERY

Blooms of the cyanobacteria *Trichodesmium* sp. occur regularly in the Great Barrier Reef and can, on occasions, extend for many hundreds of kilometres along the Queensland coast from the shoreline to the outer reef [Furnas, 1992; Revelante and Gilmartin, 1982]. *Trichodesmium* has some unique spectral characteristics that easily make it discernable from other blooming species and help its detection by ocean colour remote sensing [Sarangi et al., 2005; Subramaniam and Carpenter, 1994; Subramaniam et al., 2002]. Parts of these characteristics are accessory pigments that absorb light at different wavelengths in comparison to other species and the occurrence of blooms at the very surface of the water, often during calm sea conditions, which results in a high reflectance in satellite imagery due to the backscatter of their gas vacuoles [Subramaniam and Carpenter, 1994].

Abrupt changes of reflectance in the red (680 nm) and near-infrared (708nm) region of the spectrum make them discernable in MERIS imagery. The use of a composite of the MERIS bands at 775nm, 705nm and 681 nm and an appropriate stretching technique has proven great results (L. Metsamaa, Tartu University, Estonia; Figure 30). The positive slope between the two MERIS 681 and 705nm wavebands (Figure 31) was used to identify *Trichodesmium* affected pixels in the MERIS imagery.

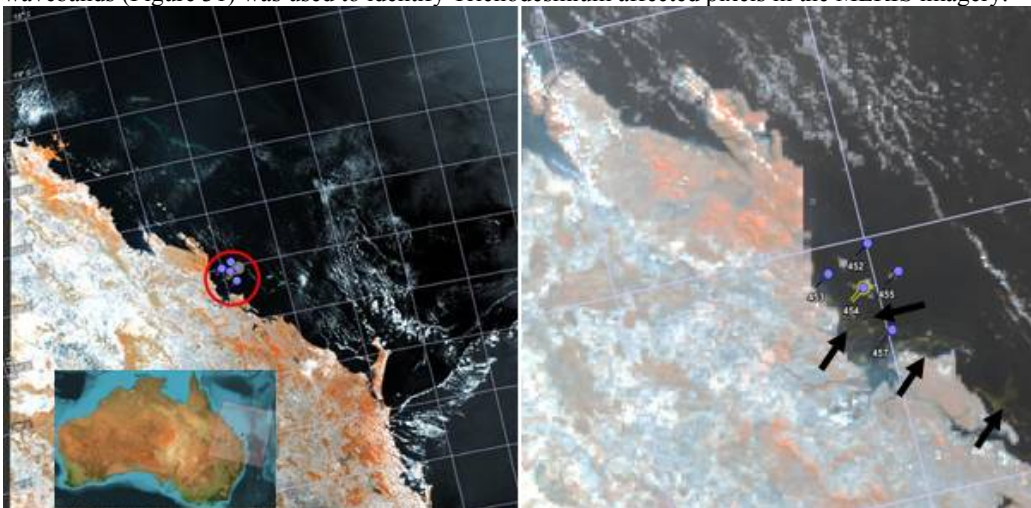


Figure 30 MERIS L1 reduced resolution (i.e., 1 pixel = 1 km) composites of bands 775nm, 705nm and 681 nm showing the locations of five stations sampled near the Fitzroy estuary on 6th October 2004 (red circle, left panel). After applying a Gaussian stretch on the same image, the long, brown filaments are *Trichodesmium* sp. become visible (right panel). Stations codes are shown.

These spectral features, as well as additional criteria [e.g., Subramaniam et al., 2002], should be used to systematically map these blooms in future work on MERIS imagery. The same method cannot be applied directly to MODIS imagery as MODIS lacks the spectral bands at 705nm that is crucial for this identification. Hence an operational algorithm to identify *Trichodesmium* affected pixels for MODIS imagery should be developed and implemented and then an inversion algorithm to estimate chlorophyll for pixels with a *Trichodesmium* expression should be developed.

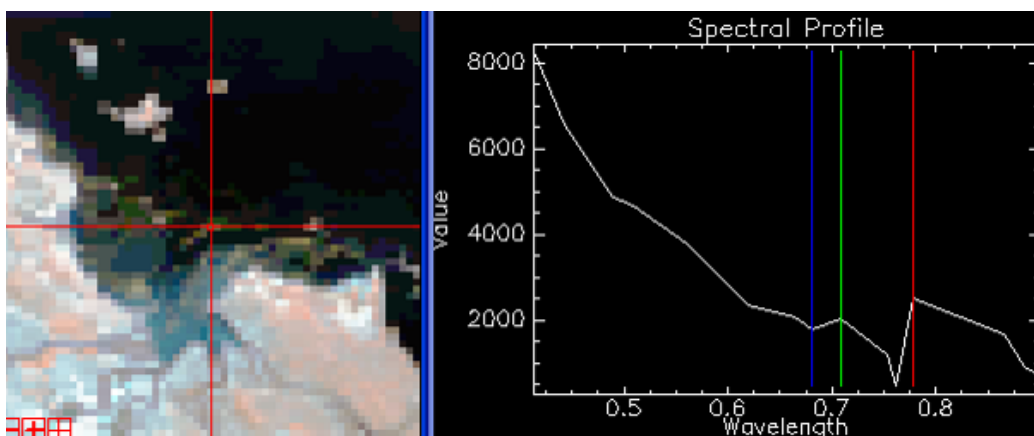


Figure 31 MERIS radiance spectrum of the studied pixel (centre of the red cross) showing a continuous decrease in radiance from 412 and 681 nm, followed by a positive slope between 681 and 705nm that identifies *Trichodesmium* sp..

References

- Furnas, M. (1992), Pelagic *Trichodesmium* (=Oscillatoria) in the Great Barrier Reef region, in *Marine Pelagic Cyanobacteria: Trichodesmium and other Diazotrophs.*, edited by E. J. Carpenter, et al., pp. 265-272, Kluwer Academic Publishers, Netherlands.
- Revelante, N., and M. Gilmartin (1982), Dynamics of Phytoplankton in the Great Barrier Reef Lagoon, *Journal of Plankton Research*, 4(1), 47-76.
- Sarangi, R. K., P. Chauhan, S. R. Nayak, and U. Shreedhar (2005), Remote sensing of *Trichodesmium* blooms in the coastal waters off Gujarat, India using IRS-P4 OCM, *International Journal of Remote Sensing*, 26(9), 1777-1780, doi:10.1080/01431160310001642340.
- Subramaniam, A., and E. J. Carpenter (1994), An empirically derived protocol for the detection of blooms of the marine cyanobacteria *Trichodesmium* using CZCS imagery., *International Journal of Remote Sensing*, 15(8), 1559–1569, doi:10.1080/01431169408954191.
- Subramaniam, A., C. W. Brown, R. R. Hood, E. J. Carpenter, and D. G. Caponea (2002), Detecting *Trichodesmium* blooms in SeaWiFS imagery, *Deep-Sea Research II*, 49, 107-121, doi:10.1016/S0967-0645(01)00096-0.
- Brando, V.E., & Dekker, A.G. (2003). Satellite hyperspectral remote sensing for estimating estuarine and coastal water quality. *IEEE Trans.Geosci.Remote Sens.*, 41, 1378-1387
- Brando, V.E., Blondeau-Patissier, D., Dekker, A.G., Daniel, P.J., Wettle, M., Oubelkheir, K., & Clementson, L. (2006a). Bio-optical variability of Queensland coastal waters for parameterisation of coastal-reef algorithms. . In, *Ocean Optics XVIII* (p. CD rom). Montreal (Canada): ONR-NASA
- Brando, V.E., Dekker, A.G., Marks, A., Qin, Y., & Oubelkheir, K. (2006b). *Chlorophyll and Suspended Sediment Assessment in a Macro-Tidal Tropical Estuary Adjacent to the Great Barrier Reef: Spatial and Temporal Assessment Using Remote Sensing.* (p. 114) Indooroopilly, Qld, Australia: CRC for Coastal Zone, Estuary and Waterway Management
- Brando, V.E., Robson, B.J., Cherukuru, N.R.C., Dekker, A.G., & Webster, I.T. (2007). Toward assimilation of ocean colour satellite observation into coastal ocean biogeochemical models: the tropical Fitzroy River Estuary case study. In *Proceedings of Assimilation of Remote Sensing and In*

Situ Data in Modern Numerical Weather and Environmental Prediction Models. (pp. 66850D-66858). San Diego, CA, USA: SPIE

Brando, V.E., Dekker, A.G., Schroeder, T., Park, Y.J., Clementson, L.A., Steven, A., & Blondeau-Patissier, D. (2008). Satellite retrieval of chlorophyll CDOM and NAP in optically complex waters using a semi-analytical inversion based on specific inherent optical properties. A case study for Great Barrier Reef coastal waters. In Proceedings of *Ocean Optics XIX*. (p. 0445). Barga, Italy

Carder, K.L., Chen, F.R., Lee, Z., Hawes, S.K., & Cannizzaro, J.P. (2003). *MODIS Algorithm Theoretical Basis Document ATBD 19*. (p. 67pp)

Giardino, C., Brando, V.E., Dekker, A.G., Strombeck, N., & Candiani, G. (2007). Assessment of water quality in Lake Garda (Italy) using Hyperion. *Remote Sensing of Environment*, *109*, 183-195

Gordon, H.R., Brown, O.B., Evans, R., Brown, J., Smith, R.C., Baker, K.S., & Clark, D.C. (1988). A semianalytical model of ocean colour. *J.Geophys.Res.*, *93(D9)*, 10909

Hoge, F.E., & Lyon, P.E. (1996). Satellite retrieval of inherent optical properties by linear matrix inversion of oceanic radiance models - an analysis of model and radiance measurement errors. *Journal of Geophysical Research-Oceans*, *101*, 16631-16648

Hoogenboom, H.J., Dekker, A.G., & De Haan, J.F. (1998). Retrieval of chlorophyll and suspended matter in inland waters from CASI data by matrix inversion. *Canadian Journal of Remote Sensing*, *24*, 144-152

Lyon, P., & Hoge, F. (2006). The Linear Matrix Inversion Algorithm. In Z. Lee (Ed.), *IOCCG Report Number 5. Remote Sensing of Inherent Optical Properties: Fundamentals, Tests of Algorithms, and Applications* (pp. 49-56). Dartmouth, Canada: IOCCG

Maritorena, S., Siegel, D.A., & Peterson, A.R. (2002). Optimization of a semianalytical ocean color model for global-scale applications. *Appl.Opt.*, *41*, 2705-2714

Qin, Y., Dekker, A.G., Brando, V.E., & Blondeau-Patissier, D. (2007). Validity of SeaDAS water constituents retrieval algorithms in Australian tropical coastal waters. *Geophys. Res. Letters*, *34*

Schaffelke, B., Carleton, J., Zagorskis, I., Furnas, M.J., Skuza, M., Wright, M., Dekker, A.G., Blondeau-Patissier, D., & Brando, V.E. (2006). *Nearshore marine water quality monitoring. In: CRC Reef Consortium. Water Quality and Ecosystem Monitoring Programs–Reef Water Quality Protection Plan. Final Report August 2006 (revision November 2006).* (pp. 105-170) Townsville: CRC Reef Research

Schroeder, T., Brando, V.E., Cherukuru, N.R.C., Clementson, L.A., Blondeau-Patissier, D., Dekker, A.G., Schaale, M., & Fischer, J. (2008). Remote sensing of apparent and inherent optical properties of Tasmanian coastal waters: application to MODIS data. In Proceedings of *Ocean Optics XIX*. (p. 0445)

Wang, P., Boss, E.S., & Roesler, C. (2005). Uncertainties of inherent optical properties obtained from semianalytical inversions of ocean color. *Applied Optics*, *44*, 4074-4085